NASA

Technical Memorandum 82088

One-Dimensional Models of Quasi-Neutral Parallel Electric Fields

David P. Stern

FEBRUARY 1981

National Aeronautics and
Space Administration

Goddard Space Flight Center
Greenbelt, Maryland 20771

ONE-DIMENSIONAL MODELS OF QUASI-NEUTRAL PARALLEL ELECTRIC FIELDS

David P. Stern
Planetary Magnetospheres Branch
Goddard Space Flight Center
Greenbelt, Maryland 20771

February 1981

Abstract:

Parallel electric fields can exist in the magnetic mirror geometry of auroral field lines if they conform to the quasi-neutral equilibrium solutions first suggested by Alfvén and by Persson. Such solutions may contain double-layer discontinuities, reflecting the disparity between the two sources which contribute to their plasma population--the hot and rarefied magnetosphere, magnetically confined, and the cool dense ionosphere, held down by gravity. This study reviews previous results on quasi-neutral equilibria and on double layers, and then examines the effects on such equilibria due to non-unique solutions, potential barriers and field aligned current flows, using as inputs monoenergetic isotropic distribution functions. Among the conclusions reached: (1) Double layer solutions not involving any net current flow are readily constructed; (2) Such layers may occur naturally and may involve a significant fraction of the total field aligned voltage drop; (3) Non-uniqueness of quasi-neutral solutions must be utilized to determine the position of such layers; (4) The gravitational potential barrier which confronts escaping ions plays an important role and must be taken into account; (5) Outbound field aligned currents are carried primarily by precipitating electrons and only a very small fraction of them is due to ionospheric positive ions; (6) Inbound field aligned currents require an appreciable voltage to drive them, and their density is no greater than that of outbound currents; (7) Precipitation with no net $j_{\parallel}$ sets up a "thermoelectric potential" similar to the one predicted by Hultqvist. Overall, the model suggests that quasi-neutral equilibria can explain many of the observed features of field aligned currents and of their associated electric fields, though solutions at this stage do not extend to voltages exceeding 2.2 kV.

Contents

1. INTRODUCTION

Until the early 1970s physicists studying the Earth's magnetosphere widely believed that magnetospheric electric fields contained only a negligible "parallel component" $E_\parallel$ along the direction of the ambient magnetic field. Instead, it was generally (though not exclusively) held that, because charged particles in the magnetosphere moved easily along magnetic field lines, any $E_\parallel$ would quickly transport ions and electrons in opposite directions, and that the contributions of such particles to the electric field would quickly nullify $E_\parallel$.

There exists now convincing evidence that $E_\parallel$ does in fact occur in the Earth's magnetosphere. In particular, electrons in discrete auroras have energy distributions which suggest that they have undergone acceleration by $E_\parallel$, and beams of O^+ ions have been observed rising from the ionosphere, apparently extracted by a parallel electric field (see Torbert and Carlson, 1980; Mozer and Torbert, 1980; Gorney et al., 1981; Mozer et al., 1980; earlier literature is reviewed by Stern, 1979). It should be noted that both above examples of $E_\parallel$ are associated with a field-aligned (Birkeland) current $j_\parallel$ flowing upwards, out of the ionosphere.

Two main approaches have emerged for explaining these observations. On one hand, it has been argued that collective plasma phenomena, commonly known as "anomalous resistivity" (Papadopoulos, 1977) hamper the flow of ions and electrons in response to $E_\parallel$ and allow the source of $j_\parallel$ to maintain a finite voltage drop. The other and older approach relies on processes which maintain charge neutrality in a plasma, both those that spread out $E_\parallel$ along a flux tube in a mirror geometry (Persson, 1966) and those that concentrate it in thin transitions or so-called double layers

(Block, 1972).

In this work we the second mechanism is examined, assuming a simplified distribution function and a one-dimensional geometry (i.e. each flux tube is considered in isolation from the rest). This does not imply that "anomalous" processes might not also be present, but rather (to echo Laplace's words) that "this hypothesis was not needed" ;in fact, if collective interactions modify the distribution function appreciably, the proper way to proceed is probably to incorporate such modification in the present model (rather than introduce an "anomalous resistivity") and then derive the electric potential Φ as before from considerations of charge neutrality. Assuming a magnetic mirror configuration along which there exists a finite voltage drop, qualitatively resembling situations occuring in the magnetosphere, equilibrium solutions were sought which take into account the presence of ionospheric plasma, gravity, potential barriers and field-aligned currents, and the uniqueness of such solutions obtained was also examined.

This work extends the study of Chiu and Schulz (1978) and also [as noted in subsection (e) below] the efforts of Lemaire and Scherer, Lennartsson and Knight. Up to a limiting value of about 2.2 kV a unique solution was always found to exist, and the voltage drop was always shared between an extended "mirror type" $E_{\parallel}$ and an abrupt "double layer" transition, with most of the voltage drop appearing in the former. The breakdown at 2.2 kV will require additional study, and may require the addition of a "trapped" particle population (below). The prevalence of "double layers" does not preclude the possibility that with appropriate distribution functions they may be absent, as found by Chiu and Schulz (1978).

Sections 2 and 3 describe the mathematical tools for handling $E_{\parallel}$ and place the present work in the context of other research and of the relevant observational evidence. We then introduce one by one the additional factors which need be considered--uniqueness,

gravity, accessibility and loss cone flows--ending in section 6 with a model of $j_{\parallel}$, qualitatively resembling the "region 1" Birkeland currents, both for downward flowing and upward flowing currents.

2. QUASI-NEUTRAL EQUILIBRIA

a. Basic Concepts

When a plasma is immersed in a homogeneous magnetic field and a parallel voltage drop is imposed along it, ions and electrons move in a way which tends to cancel $E_{\parallel}$--in Figure 1a, ions to the right, electrons to the left.

On the other hand, when the confining field has a mirror configuration, as in the dipole field of Figure 1b, and a voltage is imposed between the middle ("equator") and the ends of each field line, $E_{\parallel}$ no longer produces such a simple unidirectional shift. While a few of the particles are shifted into the loss cone and are lost, most of them keep returning to the equator, but their mirror points are now shifted, the dependence of each particle's total speed on position is changed and the net effect of all such changes on the distribution of space charge is rather complex.

It was Persson (1963,1966; also Alfven and Fälthammar, 1963) who first pointed out that under these conditions, an equilibrium was still possible, in which the particles coexist with a nonvanishing $E_{\parallel}$. Since ions and electrons are affected by $E_{\parallel}$ in different ways, the trajectories of the two species differ, but when one integrates over the entire distribution functions, charge neutrality is still maintained at every point. Persson called this a quasi neutral (QN) equilibrium, the qualifier "quasi" serving as a reminder that the calculation has chosen to ignore the tiny net space charge needed for maintaining $E_{\parallel}$ itself.

Persson himself derived the QN equilibrium supported by a monoenergetic "almost isotropic distribution function" (AIDF), isotropic except for the loss cones in which it vanished. We shall derive this solution in subsection (c) below--in part, to introduce notation, in part to illustrate the integration scheme (which differs from Persson's and which will be used throughout this study) and to derive some characteristic features of QN equilibria.

The basic magnetic configuration will consist of one half of a closed dipole-like flux tube (Figure 2), on which points are identified by their distance s from the equatorial plane (the other half is assumed to be a mirror image and therefore does not require separate treatment). At s=L there exists a "loss surface" beyond which all particles are absorbed, and subscripts (o, L) will refer to quantities evaluated at s=0 and s=L.

Let the field intensity B grow monotonically with s, and let the "mirror ratio" be defined (as in Persson's work) by

$$\gamma(s) = B(s)/B_o$$

with $\gamma_L = \gamma(L)$. It turns out that γ (rather than s) is the most convenient variable to use along the flux tube; furthermore, its use allows the present formalism to be extended to "open" field lines extending to interplanetary space, on which distance measured along field lines is unlimited, but where B tends to an asymptotic interplanetary B_o. The electric potential Φ will be assumed to vanish at the equator (s=0, γ=1) and to have a positive value Φ_L at the loss surface.

In what follows W will denote total energy (all calculations are nonrelativistic), V initial velocity, subscripts (i, e) will refer to (ions, electrons) and ($\perp$, $\parallel$) will identify components

perpendicular and parallel to the magnetic field. If subscript zero refers to the point with $\gamma=1$, we have for ions

$$W_i = (m_i/2)\, V_{oi}^2 = (m_i/2)(v_\parallel^2 + v_\perp^2) + e\,\phi(s) \qquad (1)$$

and for electrons

$$W_e = (m_e/2)\, V_{oe}^2 = (m_e/2)(v_\parallel^2 + v_\perp^2) - e\,\phi(s) \qquad (2)$$

b. Almost Isotropic Distribution Functions

Distribution functions are most conveniently expressed in terms of the constants of motion preserved by the particles which they describe, and in the present example such variables are the energy W and the magnetic moment μ. However, any two independent functions of (W, μ) can also serve, and it is often convenient to choose as such functions the equatorial velocity components ($v_{o\parallel}$, $v_{o\perp}$). At the equator, the stably trapped ions with the smallest pitch angles are those that mirror at s=L ($v_{\parallel L}=0$) and (assuming that they exist--see below) theirs is the largest $v_{o\parallel}$, satisfying

$$v_{oi\parallel}^2(\max) = (2/m_i)\,[W_i(1 - 1/\gamma_L) + e\phi_L/\gamma_L] \qquad (3)$$

Some judgement must be excercised in using this equation: if $e\phi_L > W_i$ the lhs exceeds $(2W_i/m_i)$ and this cannot be: if that is the case, no equatorial ions reach s=L and the correct limit is clearly

$$v_{oi\parallel}^2(\max) = 2W_i/m_i \qquad (4)$$

An almost isotropic distribution function (AIDF) $F_i(v_{o\parallel}, v_{o\perp})$ for ions at $\gamma=1$ can thus be written

$$F_i = f_{oi}\,\delta(v_{o\parallel}^2 + v_{o\perp}^2 - V_{oi}^2)$$

$$0 < v_{o\parallel}{}^2 < v_{o\parallel}{}^2(\max) \qquad (5)$$

$$F_i = 0 \qquad \text{otherwise}$$

Similarly, for electrons

$$F_e = f_{oe}\,\delta(v_{o\parallel}^2 + v_{o\perp}^2 - V_{oe}^2)$$

$$0 < v_{o\parallel}^2 < v_{o\parallel}^2(\max) \tag{6}$$

$$F_e = 0 \qquad \text{otherwise}$$

where

$$v_{oi\parallel}^2(\max) = (2/m_e)[W_e(1 - 1/\gamma_L) - e\phi_L/\gamma_L] \tag{7}$$

The density of either species, at any point is

$$n = 2\pi \int F\, v_\perp\, dv_\perp\, dv_\parallel \tag{8}$$

Using this with (5) and (6), one can readily derive the equatorial densities n_{oe} and n_{oi}; charge neutrality then demands $n_{oe}=n_{oi}$, and from this it follows that a certain relationship between f_{oe} and f_{oi} (see eq. 26 below) must be satisfied.

In deriving n (for either species) at an arbitrary point along the flux tube, it is convenient to split the integration of (8) into two parts--first, integrate over $v_\perp$ to obtain a one dimensional distribution function $G(v_\parallel)$ and then derive n :

$$G(v_\parallel) = \pi \int F\, dv_\perp^2 \tag{9}$$

$$n(s) = \int_{-\infty}^{\infty} G(v_\parallel)\, dv_\parallel \tag{10}$$

In the present model, the second integration is particularly

easy to perform and to generalize; furthermore $G(v_n)$ will be needed in the analysis of "double layer" discontinuities which have to be incorporated in the model.

We next try to evaluate (9) for ions with an AIDF at some given value of s. The conservation of energy, which earlier gave the bounds of v_{oin}^2 at s=0, can similarly give the bounds of v_n^2 at any other s, and the result (at all levels of this study, each of which may use different bounds) takes the form

$$v_n^2(\min) < v_n^2 < v_n^2(\max) \tag{11}$$

Using (1), eq. (9) now becomes

$$G_i(v_n, s) = \pi f_{oi} \int \delta[v_n^2 + v_\perp^2 + (2e/m_i)\phi(s) - V_{oi}^2]\, dv_\perp^2 \tag{12}$$

It follows that

$$G_i(v_n, s) = \pi f_{oi}$$

$$v_n^2(\min) < v_n^2 < v_n^2(\max) \tag{13}$$

$$G_i(v_n, s) = 0 \qquad \text{otherwise}$$

Thus the dependence of $G(v_n, s)$ on v_n is that of a slab distribution ("boxcar") and is readily integrated to

$$n_i(s) = 2\pi f_{oi} \, [v_n(\max) - v_n(\min)] \tag{14}$$

The factor 2 arises because v_n may either range over positive values from $v_n(\min)$ to $v_n(\max)$, or over negative values from $-v_n(\min)$ to $-v_n(\max)$. The first distribution represents downflowing ions, the second one ions which rise after having undergone mirroring; each of these contributes equally to n_i.

Similarly, for electrons

$$n_e(s) = 2\pi f_{oe} [v_n(max) - v_n(min)] \qquad (15)$$

Superficially, this resembles (14), but one ought to note that in general f_{oe} differs from f_{oi} and that furthermore the limits on v_n^2 (which we have chosen not to encumber with additional indices) differ for both species.

c. Persson's Solution

If the ionospheric plasma source is ignored, the boundary conditions which constitute the input of the problem are the two distribution functions (F_i, F_e) and the total voltage drop $\phi(L)=\phi_L$ between s=0 and s=L; (F_i, F_e) must be such that $n_i=n_e$ at s=0, and both densities must vanish at s=L. What is not yet determined is the detailed voltage profile, given by the function $\phi(s)$, although it is precisely that profile which determines the densities in (14) and (15).

The question raised by Persson (and before that, by Alfven and Fälthammar [1963], whose eq. (13), sect. 5.1.3, is analogous to (28) here) was whether among the many possible profiles of $\phi(s)$ there existed any for which the plasma was neutral. Both n_e and n_i depend on ϕ, and hence the neutrality condition may be formally stated as

$$n_e[s,\phi(s)] = n_i[s,\phi(s)] \qquad (16)$$

This may be viewed as the equation defining the profile $\phi(s)$ necesary for QN equilibrium. In most cases, e.g. when Maxwellian distributions are used or where several populations are superposed (Chiu and Schulz, 1978), the functional form of (16) is so complex that it can only be handled by numerical methods. In the present case, however, an analytical solution may be derived as follows.

Following the notation of Persson (1966), auxiliary functions

$\alpha(s)$ and $\beta(s)$ (not Euler potentials), depending on both $\gamma(s)$ and $\phi(s)$, are introduced as

$$\alpha(s) = [W_e + e\phi(s)]/W_e\gamma(s) \tag{17}$$

$$\beta(s) = [W_i - e\phi(s)]/W_i\gamma(s) \tag{18}$$

Since $\phi(0)=0$, $\gamma(0)=1$, it follows that

$$\alpha(0)= \beta(0)=1 \tag{19}$$

Conservation of energy now gives

$$\gamma\alpha W_e = m_e(v_n^2 + v_\perp^2)/2 \tag{20}$$

Narrowing our attention to only those electrons that mirror at $s=L$

$$\gamma_L\alpha_L W_e = m_e\, v_{L\perp}^2/2 = m_e\, v_\perp^2\, (\gamma_L/\gamma)/2 \tag{21}$$

Hence, for electrons anywhere

$$(m_e/2)\, v_n^2(\max) = \gamma(s)(\alpha - \alpha_L)W_e \tag{22}$$

Similarly, for ions

$$(m_i/2)\, v_n^2(\max) = \gamma(s)(\beta - \beta_L)W_i \tag{23}$$

We shall assume here that for any s and for both species $v_n^2(\min)=0$, i.e. that at any s there exist particles of both species which mirror locally. With the polarity assumed here, this always holds true for ions (provided that they can reach s at all), but it may fail for electrons, which are accelerated downwards by E_n. It could happen, in principle, that the v_n of electrons is increased by E_n faster than it is diminished by the conservation of μ (by the "mirror force"), so that local mirroring of electrons does not take place, and if this state of affairs

persists all the way to the loss surface, then all such electrons are lost. To avoid this possibility it must be assumed here (and may be confirmed later by examining the solutions) that E_w is everywhere sufficiently weak to prevent this from happening.

Charge neutrality implies

$$n_e^2(s) = n_i^2(s) \tag{24}$$

Substitution of (14), (15), (22) and (23) then gives, after cancellations

$$f_{oe}^2 (W_e/m_e) [\alpha(s) - \alpha_L] = f_{oi}^2 (W_i/m_i) [\beta(s) - \beta_L] \tag{25}$$

Substituting (19) here gives the relationship between f_{oe} and f_{oi} required for neutrality at s=0:

$$f_{oe}^2 (W_e/m_e) [1 - \alpha_L] = f_{oi}^2 (W_i/m_i) [1 - \beta_L] \tag{26}$$

From the last two relations it follows that

$$[\alpha(s) - \alpha_L]/[1 - \alpha_L] =$$

$$= [\beta(s) - \beta_L]/[1 - \beta_L] \tag{27}$$

Using (17) and (18) to isolate $\phi(s)$ then gives

$$\phi(s) = \phi_L [\gamma(s) - 1]/[\gamma_L - 1] \tag{28}$$

or

$$\phi_L - \phi(s) = [\phi_L/(\gamma_L - 1)] [\gamma_L - \gamma(s)] \tag{29}$$

Thus the electrical potential varies linearly with γ and with the magnetic intensity B.

d. Implications and Applications

Two properties characterize the "Perssonian" solutions obtained above. First, $E_{\parallel}$ is exactly proportional to the parallel component of ∇B (i.e. to $\partial B/\partial s$) and hence to the "mirror force" which maintains μ constant. Because of this, QN equilibria are sometimes said to involve a balance between the mirror force and the force due to $E_{\parallel}$ (e.g. Alfvén and Fälthammar, 1963).

Secondly, the plasma density n in this solution peaks at the equator, decreases linearly with increasing $\gamma(s)$ and equals zero when $\gamma=\gamma_L$. This leads to a serious question: if one extends this model by adding a cold dense ionosphere at s=L, is it possible to bridge these two dissimilar plasmas by a smooth continuous profile of n(s) and $\Phi(s)$ and still maintain quasi-neutrality? This has been one of the key issues of the present study, and as will be seen, the force of gravity must then be included to preserve the high density of the medium below.

A casual observer may object that the parallel electric field sustained by a QN equilibrium is the result of an unequal and anisotropic pitch angle distribution of magnetically confined particles and that as such particles are scattered by collisions and by collective plasma processes and become increasingly isotropic and maxwellian, such $E_{\parallel}$ would rapidly decay.

There does in fact exist an anisotropy in all models discussed here, due to the existence of a loss cone (just as it does for any mirror-confined plasma), but this is not the usual source of $E_{\parallel}$. One might consider, in principle, a "static" $E_{\parallel}$ sustained by an initial disparity between F_i and F_e, without any continuous injection of new particles or energy, and such an $E_{\parallel}$ would indeed decay; in fact the plasma itself would ultimately escape through the loss cone, as observed in mirror machines. In the magnetosphere, however, most sources of $E_{\parallel}$ are "dynamic" rather than "static," resembling a battery rather than a charged

capacitor and imposing boundary conditions which tend to maintain a finite voltage drop $\Phi_L - \Phi(0)$ in spite of a constant drain of plasma and energy. Four examples of such sources of E_n are described below, and at least 3 of these are of the "dynamic" type.

i. "Decoupling"

Observations of the geomagnetic tail have sometimes detected large-scale plasma flows at velocities of the order of 1000 km/sec, not accompanied by corresponding effects in the ionosphere (Coroniti et al., 1978). Such decoupling between distant regions and the ionosphere is one way by which E_n may be produced. Assuming for simplicity that the electric field can be represented by a scalar potential Φ and that Φ changes in distant regions but not in the ionosphere, then a gradient of Φ along the field line must exist, and this is indeed possible if a QN equilibrium can be established. The mirroring plasma in this case serves as a buffer, shielding the inner regions from rapid potential changes in the outlying ones. Of course, such buffering could also arise with inductive fields, except that now Φ may no longer be used.

Note that except for momentary overflows near the edge of the loss cone, there exists no need for net field-aligned currents in this case.

ii. "Thermoelectric" E_n

It may happen that the loss cone is filled, i.e. that the distribution function for trajectories inside it has about the same value as it has for those adjoining it. Such filling may result either from scattering in the source region $\gamma=1$ or from the arrival of fresh plasma, convected from adjoining field lines where loss processes have not yet depleted the loss cone (e.g. plasma on freshly merged field lines in the polar cusp).

In all such cases both electrons and ions are precipitated, but if ion and electron energies are comparable, the current carried by the faster electrons will greatly exceed the ion current. If no provision for closing this current exists, the ionosphere will acquire a negative potential and electrons will be extracted from it, until in equilibrium the net current vanishes. This mechanism was first proposed by Hultqvist (1970, 1971) and was further studied by Lemaire and Scherer (1974).

If no processes replenish the hot plasma population at $\gamma=1$, then this $E_{\parallel}$ is "static" and will gradually decay, as collisions and wave-particle interactions drive particles into the loss cone. In particular, the positive potential existing at $\gamma=1$ will encourage instabilities which precipitate ions, an effect which has been blamed for poor plasma containment in mirror machines and which is further discussed in subsection (2-e). On the other hand, if the loss cone is continually refilled by convection (as in the example of the cusp, above), this type of $E_{\parallel}$ is expected to maintain itself.

A similar effect is also important whenever the circuit is closed and a finite $j_{\parallel}$ is maintained. If a moderate $j_{\parallel}$ flows from the ionosphere outwards, it is only necessary to reduce the outflow of ionospheric electrons from the preceding case, and it is possible for $j_{\parallel}$ to be actually opposed to $E_{\parallel}$. A larger value of $j_{\parallel}$ may have $E_{\parallel}=0$, so that no electrons are extracted and all the current is due to the loss cone, while still higher current densities require $E_{\parallel}$ in the same direction.

When $j_{\parallel}$ flows earthwards, on the other hand, the voltage drop must exceed its zero-current equilibrium value, so that the current of electrons driven out from the ionosphere exceeds the precipitating current. All these situations are analyzed quantitatively in section 6 below and the results are summarized in Table 5.

iii. "Divergence of E"

If the magnetosphere is "open" and a bundle of polar field lines extends into interplanetary space--a situation believed to exist at least part of the time--then a voltage will exist across those lines. The reason lies with the flow of the solar wind, which produces (as viewed from the frame of the Earth) an interplanetary electric field of about 10 kV/R_E. Open field lines then tend to transmit this voltage to the polar ionosphere and a dawn-to-dusk voltage of the order of 50 kV (somewhat less than might be expected--see Stern, 1977, sect. 4c) is in fact observed in the ionosphere across the polar caps.

Because the polar ionosphere is an electrical conductor, this voltage produces a current flowing across it from dawn to dusk, and this current will be completed by Birkeland current sheets along the flanks of the polar cap, as shown schematically in Figure 3 (for the sake of simplicity, the effects of the ionospheric Hall conductivity are neglected here; such effects require departure from the simple 2-dimensional model of Figure 3, but lead to no qualitative differences). These current sheets seem to follow the "region 1" flows observed by the Triad satellite (Zmuda and Armstrong, 1974; Iijima and Potemra, 1976).

To the lowest approximation, the observed $\underline{E}$ is uniform across the polar cap, and $j_{\parallel}$ associated with it flows only from the polar cap's flanks. Such behavior requires that the voltage distribution in the source region CD (Figure 3) be uniform, for then a constant current j along AB in the ionosphere will create also there a uniform electric field $\underline{E}$ (of about 20 volt/km), and no voltage drops will exist along A'C' or A"C".

If field lines were perfect conductors, then the sheets AC and BD would indeed be infinitely thin and the above picture could be valid. Actually, however, $j_{\parallel}$ is limited to the order of 1 $\mu A/m^2$, so that the sheets are spread over a width AA' of about 200 km, as

is shown by observations (Iijima and Potemra, 1976, Figures 1; the reasons for this limitation are explored in section 6 below). By our hypothesis of a uniform source field, there exists in the source region a voltage drop CC' of about 4000 volts across each sheet. However, the drop AA' is of an order only half as large, because $j_\perp$ diminishes gradually along AA' and by Ohm's law, so does $E_\perp$. Thus parallel voltage drops of up to 2000v will arise along $j_\parallel$, where they are (presumably) maintained by a QN equilibrium.

The above is very similar to a process proposed by Lyons (1980, 1981), by which $E_\parallel$ was attributed to "the divergence of $\underline{E}$." A feature of that theory is that it predicts a gradual change in the magnitudes of both $E_\parallel$ and $j_\parallel$ across the thickness of the current sheet. Observations of $E_\parallel$ (Mozer and Torbert, 1980) suggest such a variation exists, but they should be treated with caution since they are indirect and represent averaged results from many passes. Single-pass profiles of $j_\parallel$ (Iijima and Potemra, 1976, Figures 1) suggest that the magnitude of $j_\parallel$ is relatively constant across the sheet.

iv. "Charge Separation"

The dominant flow of plasma into the vicinity of the Earth takes place from the tail and requires large-scale electric fields oriented from dawn to dusk, perhaps a combination of quiet-time fields related to the average magnetospheric convection and transient fields related to substorms (Stern, 1977 and ref.).

Now a strict $\underline{E}\times\underline{B}/B^2$ drift acts equally on ions and on electrons and does not create a net space charge. This does not hold true, however, for magnetic drifts (curvature and gradient) which, when acting on particles convected from the tail, move ions towards dusk and electrons towards dawn. This tends to produce charge separation and was first studied by Schield et al. (1969), who proposed the mechanism as a source of field-aligned currents and

who also noted the existence of "Alfven layers" accessible only to particles of one sign.

The process is complicated by time dependence and by other features (Wolf, 1975), but there seem to exist strong indications that some such type of "charge separation" is indeed the cause of "region 2" currents reported by Iijima and Potemra (1976), which occur at lower latitudes than those of "region 1" (preceding subsection), peak near midnight and are greatly enhanced during high magnetic activity. Such charge separation might well cause the parallel voltages inferred from observations of energetic ions (Ghielmetti et al., 1978; Gorney et al., 1981) in the morning sector and near midnight. The parallel voltages associated with such currents will be further discussed in section 8, after some relevant models have been developed.

e. Relation to Other Work

While the work of Alfvén and Fälthammar (1963) and of Persson (1963, 1966) attracted only limited attention, some further calculations along this direction have been published. They include the work of Lemaire and Scherer (1974, 1978), Lennartsson (1976, 1977, 1978, 1980) and of Chiu and his co-workers (Chiu and Schulz, 1978; Chiu, Cornwall and Schulz, 1980; Chiu and Cornwall, 1980). In addition, Knight (1973) assumed such that such equilibria existed and proceeded to derive the contributions to j_n from the various particle species and their dependence on the total potential drop. Several workers have applied the concepts of QN equilibrium to other matters, notably Whipple (1977) who used them in the analysis of pitch angle distributions and Lyons et al. (1979) who used some results by Knight (1973) to argue that the energy flux density of the discrete aurora should vary as the square of the accelerating voltage, in agreement with some observations; this matter has also been studied by Fridman and Lemaire(1980). Lyons (1980, 1981) also implied QN equilibria in his model of E_n, discussed in subsection (d-iii) above.

In an independent development, QN electric fields have become important to the design of magnetic mirror machines for the containment of fusion plasma (Cohen et al., 1980). In simple mirror machines there always exists a loss cone, through which some particles escape: in analogy with the "thermoelectric potential" of (2-d-ii), this raises the mirror plasma to a positive "ambipolar potential" caused by the preferential loss of electrons, a potential which in its turn slows down the loss of electrons but promotes instabilities which lead to ion loss. In the tandem mirror geometry (Coensgen et al., 1980; Schwartzschild, 1980), proposed independently by Fowler and Logan (1977) and by Dimov et al. (1976), this liability is turned into an asset: the main mirror confinement cell is joined at each end to a small auxiliary mirror cell containing relatively hot plasma, which attains a relatively high positive potential, and the result is that "end losses from (the) center cell are reduced by (the) electrostatic end-plug barrier of positive potential, which turns back those low-energy ions which escape through the magnetic mirror" (Coensgen et al., 1980).

All these calculations assumed the presence of a conducting ionosphere, but among those that derived voltage profiles, some found evidence for "double layers" while others did not. Lemaire and Scherer (1978) obtained such a layer numerically and Lennartsson (1978) argued that it was impossible to avoid doing so, although later (Lennartsson, 1980) he changed his view to maintain that QN equilibria in general were unstable. On the other hand, Chiu and Schulz (1978), using a rather elaborate numerical simulation, published profiles (loc. cit., Figs. 4 and 5; also Chiu and Cornwall, 1980, Fig. 3) which were free from discontinuities. However, their solutions are not necessarily unique, and the authors themselves have stressed (loc. cit., p.639) that "..our model is not intended to exclude the possible existence of double layers or electrostatic shocks. Indeed, it is quite easy to obtain in our model a 'solution' which has the characteristics of a double layer... However, such a potential

distribution does not satisfy our accessibility criterion.."

The present study is close in spirit to the work of Chiu and Schulz (1978) but it stresses some points not considered by those authors, while other features are simplified. Specifically, Chiu and Schulz used realistic bi-maxwellian distributions of ionospheric and magnetospheric electrons and ions, and they also included scattered and "trapped" populations and the effect of gravity. However, they did not consider the uniqueness of their solutions, and they selected only such solutions that satisfied an "accesibility criterion", meaning that whenever particles with certain conserved properties (e.g. μ and W) had access to two points (A,B) on a field line, they also had access to all points in between (accessibility is absent if a potential barrier exists between A and B, so that a (μ,W) particle moving from A to B is turned back at some in-between point). The existence of complete accessibility simplifies the calculation, but there is no compelling reason to expect it to hold in nature.

In the present study the distribution functions are greatly simplified: a magnetospheric AIDF is used having $W_i=W_e=2$ keV at s=0, while another one, for ionospheric particles at s=L, has $W_i=W_e=0.25$ ev; there exist no trapped or backscattered populations.

On the other hand, this work traces the full range of solutions of (16) and exploits their non-uniqueness to satisfy constraints due to double-layer type discontinuities. It also explores the effect of a potential barrier at low altitudes, caused by gravity, which interferes with accessibility. Finally, situations are studied where the loss cone is not empty and field-aligned currents flow. The aim has been not to create a realistic model, but to explore the qualitative features of QN equilibria and by doing so, gain insight into the processes involved and thus pave the way to more elaborate treatments.

The present calculation ignores the small charge densities (n_i', n_e') required by Poisson's equation for maintaining $E_\parallel$. These charges can in principle be taken into account by the following recursion scheme. First, using the QN approximation (16), calculate the zero-order voltage profile $\Phi_{init}(\gamma)$, in the manner derived in this study. Then, using Poisson's equation, derive $n_i'(\gamma)$ and $n_e'(\gamma)$, and with them proceed to solve a modified version of (16)

$$n_i(\Phi,\gamma) - n_e(\Phi,\gamma) = n_i'(\gamma) - n_e'(\gamma)$$

This is probably best handled by expanding Φ

$$\Phi(\gamma) = \Phi_{init}(\gamma) + \Phi'(\gamma)$$

and solving for the small correction Φ'. Because of Poisson's equation, Φ' will next require small corrections to be added to (n_i', n_e'), which in turn produce a further correction to Φ. Assuming the process converges, Φ may thus be derived to an arbitrary accuracy.

However, the fact that the present study is strictly one-dimensional, with each flux tube considered completely apart from those adjoining it, introduces a basic flaw into this scheme. In the polar regions of the Earth, where $E_\parallel$ is important, there also exists a considerably larger convection field $\underline{E}_\perp$. As noted by Chiu and Cornwall (1980; top of col.2, p.546) the free charge densities (n_i', n_e') required to satisfy Poisson's equation then consist of two parts, one related to $E_\parallel$ and the other to $\underline{E}_\perp$, and the latter part completely overshadows the former: while $E_\parallel$ alone would require $n'/n \sim 10^{-8}$, $\underline{E}_\perp$ requires $n'/n \sim 10^{-2}$–10^{-3}. Because of this the errors corrected by our recursion scheme are far smaller than those introduced by the assumption of one-dimensionality and left uncorrected.

Practically, of course, n'/n in either case is small enough to suggest that (16) will indeed yield a rather good approximation to

$\phi(\gamma)$.

The next section is devoted to an exposition of some models of double layers, used in this study. Beginning with section 4 the various features listed above are added to Persson's simple model one by one and the results are discussed and evaluated.

3. DOUBLE LAYERS

a. Definition

It is an indication of the controversial nature of double layers that opinions are divided even about their definition (Kan, 1980). This study will use the following definition:

> "A double layer is a discontinuity of the electric field, resulting from the tendency (or loosely,'desire') of the plasma to maintain charge neutrality in the regions which adjoin it."

While Kan (1980, 2nd para.) has stated that "the electric current is an essential element in a double layer," the above definition does not postulate any current flow (in common with a definition used by Block, [1978]; a similar attitude is expressed by Carlqvist, [1979], and in a recent work by Perkins and Sun [1981]). Indeed, j_n vanishes in all models investigated here except for those of section 6, yet "double layer" discontinuities are found to exist in all cases. Nor do current-free configurations represent artificial situations which are not likely to arise in nature, since two of the examples of subsection (2-d) above do not require any currents.

A simple example will illustrate the meaning of "...the tendency of plasma to maintain charge neutrality" (Figure 4). Consider the space between two planar plasma sources A and B,

threaded by a common flux tube of a magnetic field $\underline{B}$ (or alternatively, $\underline{B}=0$: in either case no magnetic forces affect the plasma), and let each source be able to supply an unlimited number of particles of either sign. A voltage generator is now connected between A and B, capable of delivering a total current I and producing a voltage difference ϕ_{AB} between its terminals whenever such a current is generated. What will be the equilibrium potential profile $\phi(s)$ between A and B under these conditions?

With the voltage polarity shown, ions are emitted from A and electrons from B: to simplify matters, it will be assumed that all particles of each kind start out with the same speed along AB, so that at any distance s from the source A all ions and all electrons have unique speeds $v_i(s)$ and $v_e(s)$. If $n_i(s)$ and $n_e(s)$ are the corresponding densities, it is easy to see that no equilibrium can exist in which charge neutrality holds everywhere. For by the equation of continuity

$$n_i(s)\ v_i(s) = \text{const.} \qquad (30)$$

and hence

$$v_i(s)\ [dn_i/ds] + n_i(s)\ [dv_i/ds] = 0 \qquad (31)$$

Similarly

$$v_e(s)\ [dn_e/ds] + n_e(s)\ [dv_e/ds] = 0 \qquad (32)$$

Thus dv_i/ds and dn_i/ds must have opposite signs, and so must dv_e/ds and dn_e/ds. However, since the electric field accelerates ions and electrons in opposite directions, dv_i/ds and dv_e/ds are of opposing sign, so that dn_i/ds and dn_e/ds also differ in sign, i.e. the two densities must increase in opposite directions. But then the neutrality requirement $n_i(s)=n_e(s)$ for any s cannot be satisfied.

Consequently a net space charge must exist at least in part of the region. Since even a modest space charge requires a rather substantial electric field, this range will tend to be quite small. In the final equilibrium $\underline{E}$ vanishes throughout most of the space between A and B, and only over a narrow thickness

$$s_{DL} < s < s_{DL} + d \qquad (33)$$

is the plasma non-neutral. Thin plasma structures of this type are usually known as sheaths (especially when they occur near conducting boundaries), but in space applications the term "double layer" (henceforth abbreviated to DL) has gained currency. A simple model of such a layer derived by Block (1972, eqs. 1) clearly shows that given a finite voltage drop Φ_{AB}, such a structure can accomodate a wide range of current density j by adjusting its thickness d: thus it is misleading to discuss the "resistance" of a DL. Additional details and more elaborate models will be developed below.

Many studies exist about double layers and other abrupt transitions of the electric field, and the reader is referred to reviews and articles by Block (1972, 1978), Goertz (1979), Carlqvist (1979), Levine and Crawford (1979), Kan (1975), Kan and Lee (1980a,b) and Hasan and Ter Haar (1978), as well as to the numerous additional references cited by those authors. The model used here and developed in the next subsection parallels one described by Hasan and Ter Haar (1978). In addition, many laboratory experiments related to the formation of double layers have been performed, but the only one involving a mirror configuration somewhat similar to the one studied here is a recent experiment by Stenzel et al. (1980).

b. A Model Double Layer

i. Densities

All double layers considered here are one-dimensional, with the potential Φ depending only on the distance s along a magnetic field line and ignoring the effects of the curvature of such lines (i.e. $E_{\parallel} = - d\Phi/ds$). When particles confined by a magnetic field encounter such a layer, only their $v_{\parallel}$ changes, while $v_{\perp}$ (and hence μ) remain unaffected: therefore, when treating the flow of plasma through such a DL, it is permissible to use one-dimensional distribution functions similar to $G(v_{\parallel})$ of (9). Furthermore, because a monoenergetic AIDF is generally assumed, $G(v_{\parallel})$ will as a rule be a "boxcar" function, having a constant value for

$$v_{\parallel}(\min) < |v_{\parallel}| < v_{\parallel}(\max) \qquad (34)$$

and vanishing elsewhere; except for the examples of section 6, the ranges of positive and negative $v_{\parallel}$ will be the same. Rather similar assumptions are used in the first of the two models analyzed by Hasan and Ter Haar (1978), except that there some of the distribution functions are delta functions (loc. cit., eqs. 3.4), while here all functions are boxcars.

Next, a suitable notation will be introduced. In the magnetosphere each DL has a lower side, facing Earth, and a higher side, facing away: by the conventions of Figure 2, the lower side has the larger value of s and of the electric potential Φ (assuming Φ is monotonic). Quantities related to particles originating above the DL will be distinguished by subscripts "1", those originating below by subscripts "2", and subscripts (i,e) will as before denote (ions, electrons). On the other hand, the subscript "parallel" will be omitted here (in this subsection only!) and $v_{\parallel}$ will be written simply as v, since $v_{\perp}$ never appears. The initial parallel velocities with which particles arrive at either side of the layer will be denoted by V, with appropriate subscripts.

Let the layer extend over

$$s_{DL} < s < s_{DL} + d \tag{35}$$

with

$$\phi(s_{DL}) = \phi_{DL}$$
$$\phi(s_{DL}+d) = \phi_{DL} + \psi \tag{36}$$

A schematic view of the potential distribution inside the DL and of the different distribution functions involved is shown in Figure 5. Just as $\gamma(s)$ is more convenient than s for denoting position in QN equilibria, so $\phi(s)$ is the preferred variable for studying double layers. In what follows the potential of points inside the DL will be written as

$$\phi(s) = \phi_{DL} + \zeta$$
$$0 < \zeta < \psi \tag{37}$$

and $\zeta(s)$ will be used to denote position.

The structure of the DL involves four particle populations -- ions and electrons from above, having at $\zeta=0$ distribution functions

$$G_{i1}(V_{i1}) \quad \text{and} \quad G_{e1}(V_{e1})$$

and ions and electrons from below, having at $\zeta=\psi$ distribution functions

$$G_{i2}(V_{i2}) \quad \text{and} \quad G_{e2}(V_{e2}).$$

Each of these contains a pair of boxcar distributions, one for positive velocities and one for negative ones. For example, magnetospheric electrons at $\zeta=0$ have

$$G_{e1}(V_{e1}) = N_{e1}/V_{e1o} \quad \text{if} \quad V_{e1B}^2 < V_{e1}^2 < V_{e1T}^2 \tag{38}$$

$$G_{e1}(V_{e1}) = 0 \qquad \text{otherwise}$$

where subscripts (T,B) denote (top, bottom) of the range, V_{e1o} is the initial velocity of all ions at $\zeta=0$ and N_{e1} is a constant; the division by V_{e1o} is included in order to give N_{e1} dimensions of density, for by eq. (10) the density of these electrons at $\delta=0$ is

$$n_{e1}(0) = 2\, N_{e1}\, (V_{e1T} - V_{e1B})/V_{e1o} \qquad (39)$$

The factor 2 acknowledges from the existence of both positive and negative ranges of v, for although the source of G_{i1} is "above", magnetic mirroring causes equal fluxes of its electrons to traverse the DL in both directions.

At other values of ζ, it remains true that for a given value of v_{e1}, $G_{e1}(v_{e1})$ can only either vanish or equal the set value N_{e1}/V_{e10}, because its dependence (or non-dependence) on v_{e1} is the same as on V_{e1} (this may also be viewed as an example of Liouville's theorem). However, the limits (v_{e1T}, v_{e1B}) within which it differs from zero depend now on ζ. From the conservation of energy

$$\begin{aligned} v_{e1T}^2 &= V_{e1T}^2 + (2e/m_e)\zeta \\ v_{e1B}^2 &= V_{e1B}^2 + (2e/m_e)\zeta \end{aligned} \qquad (40)$$

and therefore

$$n_{e1}(\zeta) = 2(N_{e1}/V_{e1o})\, [\, (V_{e1T}^2 + (2e/m_e)\zeta)^{1/2} - (V_{e1B}^2 + (2e/m_e)\zeta)^{1/2}\,] \qquad (41)$$

Because magnetospheric electrons are accelerated throughout the double layer, there exists no possibility of a negative radicand. The situation may differ for magnetospheric ions, which are slowed down in the DL and whose density is formally

$$n_{i1}(\zeta) = 2(N_{i1}/V_{io}) \left[(V_{i1T}^2 - (2e/m_i)\zeta)^{1/2} - \right.$$

$$\left. - (V_{i1B}^2 - (2e/m_i)\zeta)^{1/2} \right] \qquad (42)$$

In the above equation, V_{i1B} is the initial velocity of the slowest ions entering the layer: if

$$(V_{i1B}^2 - (2e/m_i)\zeta)$$

is negative, then such ions will have already undergone reflection before reaching $\zeta(s)$, and at $\zeta(s)$ itself the slowest ions will be those which are reflected locally, from which it follows that $v_{i1B}=0$. This property can be expressed with the help of the Heaviside step function θ, defined by

$$\theta(x) = 1 \quad \text{if} \quad x > 0$$

$$\theta(x) = 0 \quad \text{if} \quad x < 0 \qquad (43)$$

In what follows equations will be simplified by the convention that if the argument of θ is not explicitly stated, it is understood to be the function immediately preceding θ. For example

$$[(V_{i1B}^2 - (2e/m_i)\zeta(s))\theta] \equiv [(V_{i1B}^2 - (2e/m_i)\zeta]\ \theta(V_{i1B}^2 - (2e/m_i)\zeta) \qquad (44)$$

and by the preceding discussion, this replaces the second term in (42). Similar arguments hold for the first term, and the final result is

$$n_{i1}(\zeta) = 2(N_{i1}/V_{i1o}) \left([(V_{i1T}^2 - (2e/m_i)\zeta)\theta]^{1/2} - \right.$$

$$\left. - [(V_{i1B}^2 - (2e/m_i)\zeta)\theta]^{1/2} \right) \qquad (45)$$

Note that if a "critical ζ" ζ_c exists in the DL such that

$$(2e/m_i)\ \zeta_c = V_{i1T}^2 \qquad (46)$$

then all magnetospheric ions will have undergone reflection by the time ζ_c is reached, and for $\zeta > \zeta_c$ both terms in (45) vanish, giving

$$n_{i1}(\zeta) = 0 \quad (\zeta > \zeta_c) \qquad (47)$$

In what follows the terminology of Carlqvist (1979) will be adopted and particles turned back by the electric field in a double layer will be known as "reflected" particles: the term "trapped" is often used in the literature, but here that term is used in the sense given to it by Chiu and Schulz (1978, end of p. 631), for particles confined between a low-altitude magnetic mirror and a high-altitude electric one.

Expressions entirely analogous to those derived above hold for particles originating below the layer, except that now the voltage drop traversed in reaching $\zeta(s)$ is $(\psi-\zeta)$ and the electrons rather than the ions are retarded by the field. Thus at the lower boundary

$$n_{e2}(\psi) = 2\ N_{e2}\ (V_{e2T} - V_{e2B})/V_{e2o} \qquad (48a)$$

$$n_{i2}(\psi) = 2\ N_{i2}\ (V_{i2T} - V_{i2B})/V_{i2o} \qquad (48b)$$

and inside the plasma

$$n_{e2}(\zeta) = 2\ (N_{e2}/V_{e2o})\ (\ [(V_{e2T}^2 - (2e/m_e)(\psi-\zeta))\theta]^{1/2} -$$

$$-\ [(V_{e2B}^2 - (2e/m_e)(\psi-\zeta))\theta]^{1/2}\ ) \qquad (49a)$$

$$n_{i2}(\zeta) = 2\ (N_{i2}/V_{i2o})\ (\ [V_{i2T}^2 + (2e/m_i)(\psi-\zeta)]^{1/2} -$$

$$- \left[V_{i2B}^2 + (2e/m_i)(\phi-\zeta)\right]^{1/2}) \qquad (49b)$$

Since the plasma is neutral at its boundaries

$$n_{e1}(0) + n_{e2}(0) = n_{i1}(0) + n_{i2}(0) \qquad (50a)$$

$$n_{e1}(\phi) + n_{e2}(\phi) = n_{i1}(\phi) + n_{i2}(\phi) \qquad (50b)$$

Consequently only two of the 4 density constants (N_{e1}, N_{i1}, N_{e2}, Ni_2), or two combinations of them, can be specified, and the rest is then derived from (50). For instance, it is possible to specify the total plasma densities above and below the layer (the terms on either side of the equalities in eqs. 50) and derive the 4 constants from them.

ii. The Jump Condition

In all preceding equations densities were expressed in terms of ζ, the electric potential relative to the top of the layer. To derive the voltage profile $\zeta(s)$, Poisson's equation must be used

$$d^2\zeta/ds^2 = -(e/\varepsilon_o)\,[n_i(\zeta) - n_e(\zeta)] \qquad (51)$$

Following Bernstein, Greene and Kruskal (1957), a function $V(\zeta)$ is introduced, satisfying

$$dV/d\zeta = -\,d^2\zeta/ds^2 \qquad (52)$$

Substituting this in (51) allows $V(\zeta)$ to be integrated

$$V(\zeta) - V(0) = (e/\varepsilon_o) \int_0^{\zeta} [n_i(\zeta) - n_e(\zeta)]\, d\zeta \qquad (53)$$

However, it also follows from (52) that

$$2(dV/ds) = -\,d/ds\,[(d\zeta/ds)^2] \qquad (54)$$

This may be integrated from 0 to the value of s corresponding to a given ζ; assuming that outside the layer (and hence also at its boundary ζ=0) the electric field vanishes, one finds $d\zeta/ds$=0 at ζ=0 and hence

$$2[V(\zeta) - V(0)] = -\,(d\zeta/ds)^2 \qquad (55)$$

Eq. 55 reveals the intuitive significance of V--if V(0)=0, it is proportional to E^2 and hence to the energy density of the electric field. From this the inverse function $s(\zeta)$ of the voltage profile can be recovered, using

$$s = 2^{-1/2} \int_0^{\zeta} [V(\zeta) - V(0)]^{-1/2}\, d\zeta \qquad (56)$$

and substituting from (53) in the integrand.

If the electric field E vanishes on both sides of the layer, then V=0 at both $\zeta=0$ and $\delta=\psi$, and by (53)

$$\int_0^{\psi} n_{ch}(\zeta)\, d\zeta = \int_0^{\psi} [n_i(\zeta) - n_e(\zeta)]\, d\zeta = 0 \qquad (57)$$

This is a consistency condition which must be obeyed by all double layers, stating that the total integrated charge density across the layer vanishes. The intuitive meaning of the condition is best seen if the layer is regarded as very thin: the lhs of (57), multiplied by the electron charge e, then gives the layer's surface charge density σ coulomb/m^2. According to electromagnetic theory, any discontinuous jump of the electric component orthogonal to a plane surface is proportional to the surface charge density σ: since this component is continuous (namely, zero on both sides), σ must vanish. We shall refer to (57) as the "jump condition."

At this point one may wonder whether these boundary conditions are significantly altered when the layer is embedded in a QN equilibrium, in which $E\neq 0$ ($\underline{E}$ is parallel to $\underline{B}$ but orthogonal to the layer: to avoid confusion, no subscripts are used). The answer is no: in order for the jump condition to be significantly modified, E^2 adjacent to the layer must be an appreciable fraction of E^2 inside it, and this does not occur. In this connection one may note a definition of double layers attributed to Karl Schindler (C. Goertz, private communication), according to which "double layers are regions in which the energy density of the electric field is comparable to that of the plasma particles."

In very simple cases (Block, 1972) the jump condition reduces

to the Langmuir condition, which states that the electron current through a double layer exceeds the ion current by a ratio $(m_i/m_e)^{1/2}$. In more elaborate cases, though, the jump condition becomes rather complex; furthermore, in many of the examples considered here, both the electron current and the ion current vanish, since every particle trajectory is matched by one similar in all details but with the direction of motion reversed.

With the 4 populations postulated here, (57) is resolved into 4 terms

$$Q_{DL} = Q_{i1} + Q_{i2} + Q_{e1} + Q_{e2} = 0 \qquad (58)$$

where for any index pair k

$$Q_k = q \int_0^{\psi} n_k \, d\zeta \qquad (59)$$

and where q=1 for ions and q=-1 for electrons. With the densities expressed here (eqs. 41, 45 and 49), the integrals can only have one of two forms. For Q_{e1} and Q_{i2}, all integrals are of the type

$$I_1 = \int_0^{\psi} (a + b\zeta)^{1/2} \, d\zeta = (2/3b)[(a+b\psi)^{3/2} - a^{3/2}] \qquad (60)$$

For other particles, the integrand includes a step function

$$I_2 = \int_0^{\psi} [(a - b\zeta)\theta]^{1/2} \, d\zeta \qquad (61)$$

and it is always possible to arrange for it to be finite at the upper limit (a new variable $\zeta' = \psi - \zeta$ must sometimes be introduced).

If the θ function does not equal unity over the entire range, that range must include the value

$$\zeta_c = a/b \tag{62}$$

at which the integrand vanishes. Then

$$I_2 = \int_{\zeta'}^{\psi} (a - b\zeta)^{1/2}\, d\zeta = -(2/3b)\,(a-b\psi)^{3/2} \tag{63}$$

In addition to the jump condition, there exists the so-called Bohm criterion (Bohm, 1949; Block, 1972; Kan and Lee, 1980a,b) which states (roughly) that in order for the double layer to have abrupt boundaries rather than gradual ones, the mean speed at which particles enter it must exceed (by some small factor) their thermal speed. A simplified version of this criterion can be developed for the present model (Hasan and Ter Haar, 1978, eq. 3.19) but we shall not follow this matter, other than note that the criterion might be violated in magnetospheric DLs if ionospheric particles enter them directly without any appreciable pre-acceleration.

4. SIMPLE EQUILIBRIA

a. Ionospheric Sources

The initial model assumes a flux tube (drawn schematically in Figure 6 with its curvature removed) with two pairs of particle populations: a magnetospheric plasma with densities (n_{e1}, n_{i1}) originating at the "equator" s=0, and an ionospheric plasma with densities (n_{e2}, n_{i2}) originating at s=L, which is considered as a "loss surface" for magnetospheric particles but a "source surface" for ionospheric ones.

In all models derived in this study, the initial energies of ions and electrons were chosen to coincide, being equal to 2 kev for the magnetospheric component and 0.25 ev for the ionospheric one. The plasma density at s=0 (or γ=1) was chosen as 1 cm^{-3} while the ionospheric density at s=L was varied, the most typical value being 25 cm^{-3} (only the ratio of the two densities affects the voltage profile). Finally, all calculations here assume γ_L=436 and (except at the end of section 6) a total voltage drop ϕ_L=1000v.

For magnetospheric particles (index "1")

$$v_{e1}^2 = v_{e1''}^2 + v_{e1\perp}^2 - (2e/m_e)\phi(s) \qquad (64)$$

$$v_{i1}^2 = v_{i1''}^2 + v_{i1\perp}^2 + (2e/m_i)\phi(s) \qquad (65)$$

It is assumed that at any s there always exist locally mirroring magnetospheric particles of both kinds (see comments following eq. 23), so that the smallest values of $v_{e1''}$ and $v_{i1''}$ are always zero. The largest possible parallel velocities belong to particles that mirror at s=L: if these are electrons then their perpendicular velocity at s=L satisfies

$$v_{L\perp}^2 = V_{e1}^2 + (2e/m_e)\phi_L \qquad (66)$$

and hence from (64), by conservation of μ

$$\begin{aligned} v_{e1''}^2(max) &= V_{e1}^2 + (2e/m_e)\phi - (\gamma/\gamma_L)v_{L\perp}^2 \\ &= [V_{e1}^2 + (2e/m_e)\phi_L][1-(\gamma/\gamma_L)] + \\ &\quad + (2e/m_e)(\phi - \phi_L) \end{aligned} \qquad (67)$$

For ions

$$v_{L\perp}^2 = V_{i1}^2 - (2e/m_i)\phi_L \qquad (68)$$

$$v_{i1\parallel}^2(\max) = [V_{i1}^2 - (2e/m_i)\phi_L][1-(\gamma/\gamma_L)] - \\ - (2e/m_i)(\phi - \phi_L) \qquad (69)$$

(eqs.(67) and (69) resemble (22) and (23) but the notation differs). The densities now are

$$n_{e1}(\gamma) = 2(N_{e1}/V_{e1})\, v_{e1\parallel}(\max) \qquad (70a)$$

$$n_{i1}(\gamma) = 2(N_{i1}/V_{i1})\, v_{i1\parallel}(\max) \qquad (70b)$$

where the constants (N_{e1}, N_{i1}) are defined as in (39) and (40) and are determined by the conditions that at s=0 (γ=1) the plasma is neutral and has a density 1 cm^{-3}. These conditions can be utilized only after n_{i2} is derived, as shown below.

Among ions rising from the ionosphere, the largest $v_\parallel$ belongs to those that are emitted parallel to the field, with zero pitch angle. By the conservation of μ, such ions have $v_\perp$ =0 anywhere, and consequently the conservation of energy gives, at any value of s

$$v_{i2\parallel}^2(\max) = V_{i2}^2 - (2e/m_i)(\phi(s)-\phi_L) \qquad (71)$$

The smallest value of $v_{i2\parallel}$ belongs to ions emitted with 90° pitch angle, so that for them, at s=L

$$v_{L\perp}^2 = V_{i2}^2 \qquad (72)$$

Using the conservation of W and μ then yields

$$v_{i2\parallel}^2(\min) = V_{i2}^2[1-(\gamma/\gamma_L)] + (2e/m_i)(\phi_L-\phi) \qquad (73)$$

As is evident, $v_{i2\parallel}$ is always real, since each of the right hand terms is positive, in agreement with the assumed polarity of $E_\parallel$, which accelerates ionospheric ions upwards. In contrast,

ionospheric electrons are opposed by E_n and since the total voltage drop ϕ_L=1000v greatly exceeds their initial energy of 0.25ev, they do not get very far; in fact, one may assume that at every point accessible to electrons, some of them will mirror locally, so that $v_{e2n}(min)=0$. The relations corresponding to (71) and (73) then become

$$v^2_{e2n}(max) = [V^2_{e2} + (2e/m_e)(\phi_L-\phi)]\theta \qquad (74a)$$

$$v^2_{e2n}(min) = 0 \qquad (74b)$$

where, according to the notation introduced earlier, the argument of the step function is the term preceding it. The corresponding densities are

$$n_{e2}(s) = 2(N_{e2}/V_{e2})\, v_{e2n}(max) \qquad (75a)$$

$$n_{i2}(s) = 2(N_{i2}/V_{i2})[v_{i2n}(max) - v_{i2n}(min)] \qquad (75b)$$

Here $2N_{i2}$ is the given limiting density at s=L and neutrality requires $N_{i2}=N_{e2}$. The quasi-neutrality condition then requires that at any s

$$n_{ch}(s) = n_{i1}(s) + n_{i2}(s) - n_{e1}(s) - n_{e2}(s) = 0 \qquad (76a)$$

Examination of (65), (67) and (73) shows that the excess charge density n_{ch} depends on s only through the functions $\phi(s)$ and $\gamma(s)$, so that (76a) may also be written

$$n_{ch}(\phi,\gamma) = 0 \qquad (76b)$$

Numerical solutions of (76b) are readily obtained. Choosing representative values of γ within the range $1 < \gamma < \gamma_L$, one first derives the limiting values $n_{ch}(0,\gamma)$ and $n_{ch}(\phi_L,\gamma)$, whose signs generally differ. By successive halving of the range, a solution of (74b) can then be approached as closely as is desired; more

elegant analytical iterations tend to be unreliable, because the slope of the curve sometimes changes radically within a short range of ϕ. The detailed properties of such solutions are studied in the next subsection.

b. Uniqueness and the Jump Condition

Iterative solutions of (76b) generally lead to profiles $\phi(\gamma)$ which are discontinuous, with the voltage dropping abruptly at some value of γ, typically by about 30% of ϕ_L. This suggests that double-layer type discontinuities are embedded in the quasi-neutral profile. Inside such layers quasi-neutrality does not hold, since the jump condition (57) only requires the vanishing of the integral of n_{ch}, and not of n_{ch} itself.

It turns out, however, that most iterative solutions of (16) which include a discontinuity do not fit the jump condition (57). The problem is resolved, as shown below, by noting that such solutions are not unique, and that among them a unique solution which also satisfies (57) can generally be found.

Consider the plot of $n_{ch}(\phi,\gamma)$ against ϕ, for a fixed value of γ, qualitatively shown in Figure 7 (the scales on both axes are unevenly drawn to bring out the qualitative features of the relationship, which however are the same for all values of γ). As can be seen, the curve has a "valley" and a "peak" (actually a cusp), the latter located around $\phi=(1000-0.25)$ev, the value which no ionospheric electrons can pass. Solutions of (76b) occur where this curve intercepts the line $n_{ch}=0$.

Figure 7 corresponds to a small value of γ (e.g. $\gamma=10$): the peak is submerged and a unique solution exists. At $\gamma=1$, of course, the straight line intercepts the curve at $\phi=0$, since at the equator equilibrium is assumed to exist at $\phi=0$.

As γ increases, the top of the peak approaches the line until,

at some $\gamma=\gamma_1$, the two touch (Figure 8). Beyond this value the peak juts above the line $n_{ch}=0$ and three solutions exist as shown, denoted (ϕ_1,ϕ_2,ϕ_3).

Still further increases in γ bring the line closer to the valley floor, until at $\gamma=\gamma_2$ the two make contact (Figure 9); for $\gamma>\gamma_2$ the solutions ϕ_1 and ϕ_2 disappear and only a unique solution ϕ_3 remains. As γ approaches γ_L, ϕ_3 should approach ϕ_L, as required by the boundary conditions at s=L.

Thus for $\gamma<\gamma_1$ a unique solution exists, continuous with ϕ_1, while for $\gamma>\gamma_2$ the solution is also unique and is continuous with ϕ_3. If ϕ_2 is ignored (and this will be justified below) then somewhere between γ_1 and γ_2 the solution must leap discontinuously from ϕ_1 to ϕ_3.

A straightforward numerical scheme for solving (76) generally selects the transition in an unpredictable fashion, and the jump condition

$$0 = \int_0^{\psi} n_{ch}\, d\zeta = \int_0^{\psi} (n_{i1} + n_{i2} - n_{e1} - n_{e2})\, d\zeta \qquad (57)$$

is generally not obeyed. However, a judicious choice of the transition point can indeed satisfy (57), for one finds that at γ_1, $Q_{DL}<0$, at γ_2, $Q_{DL}>0$, and in between these two extremes (in those cases that were studied) Q_{DL} varies monotonically. While the above result was first obtained by trial and error, it does in fact have an intuitive interpretation, as follows.

Suppose that Figure 10 describes the numerical solution of (76b) at the value of γ_{DL} where an abrupt transition from ϕ_1 to ϕ_3 satisfies the jump condition (57). All terms in (57) may be derived from equations such as (70) and (75), because they all depend on (γ,ϕ) in a way involving only the conservation of (W,μ), which holds both inside and outside the DL (the conservation of μ

in the DL is trivial, since neither γ not $v_\perp$ change there). For instance, $n_{11}(\zeta)$ is given by (70b), using (69) with $(\gamma_{DL},\phi_{DL}+\zeta)$ replacing there (γ,ϕ).

The appropriate formulas for other species are obtained similarly, with γ held constant and equal to γ_{DL} everywhere. Thus the quantity plotted in Figure 10 is in fact the integrand of (57), plotted against $\phi=\phi_{DL}+\zeta$. The jump condition therefore simply means that the net area bounded by the curve and the line $n_{ch}=0$ must vanish (area below the line being counted as negative). By Figures 8 and 9, this area is negative at γ_1 and positive at γ_2, hence if it is a continuous function of γ it must vanish at some intermediate value γ_{DL}, and if that function is monotonic, then γ_{DL} is unique.

Obviously, this method could be extended to equilibria with more realistic distribution functions. It also suggests that discontinuities which have $\phi=\phi_2$ at one of their boundaries can never satisfy (57), for the areas enclosed between ϕ_1 and ϕ_2, or between ϕ_2 and ϕ_3, are of one sign and can never vanish.

A model calculation was attempted, using the input parameters of subsection (4-a) and the formulas derived there. Solutions resembling those discussed above were obtained, and they are traced in Figure 11, as well as tabulated in Table 1. The jump condition was tested for various values of γ, and by means of an iterative search it was found that it was satisfied for $\gamma=183.91$.

Closer examination of the solution, however, shows that it is flawed, in that it does not match its stipulated boundary values, neither in density (where the discrepancy is appreciable) nor in potential. Thus, strictly speaking, (16) has no solution which satisfies all the conditions imposed by the problem.

In order to trace the cause of this mismatch, the densities of the various plasma components were derived for values of (γ,ϕ) very close to their boundary values (e.g. $\gamma=435.99$, $\phi=.999\ 999$).

For all such cases n_{ch} was negative, because as γ decreased from its boundary value γ_L, n_{i2} diminished much faster than did n_{e2}, an understandable result since E_n accelerated ions upwards but held back electrons. The densities of the two magnetospheric components n_{i1} and n_{e1} were extremely small (they tend to zero as γ tends to γ_L) and were not sufficient to overcome the imbalance in the charge density, so that no equilibrium could exist.

Thus the reason for the observed behavior can be traced to the uncontrolled acceleration of ions away from $\gamma=\gamma_L$, and this arises because a boundary plasma was postulated at $\gamma=\gamma_L$ without any visible means of keeping it from "floating away." In nature such means are provided by gravity; it will be shown below that after gravity is incorporated in the model, densities begin to match their boundary values, though new problems must then be addressed.

5. THE EFFECT OF GRAVITY

a. The Equivalent Potential

The lower boundary of the region of E_n is in the ionosphere, which is held down by gravity. Although the gravitational potential $m\Omega$ is much smaller than $e\Phi_L$ (the escape energy $W(\infty)$ of an O^+ ion amounts to about 10.45 ev) a consistent model must include gravity, for gravity may be dominant near $\gamma=\gamma_L$, where the externally produced E_n is rather weak.

As was first pointed out by Pannekoek (1922) and Rosseland (1924), gravity gives rise to a weak electric potential $\Phi_g(z)$, depending on the altitude z. In the auroral zone, magnetic field lines are nearly vertical and this "Pannekoek-Rosseland field" ("PR field") adds almost its entire strength to E_n; therefore Φ_g will simply be added to the field aligned potential Φ and it will be assumed that z=L-s. The effect arises as follows.

Above the thermopause (about 110 km) atmospheric density no longer follows a single scale height, but instead each species tends to taper off independently of the others. At altitudes of interest here the charged component is dominated by O^+ ions and by free electrons, with a temperature of about 3000^o (Banks and Holzer, 1969a, b), i.e. a mean energy of about 0.25 ev. If these electrons and ions were truly independent, the scale height of electrons would greatly exceed that of ions--in fact, most electrons would escape completely. However, charge neutrality requires that both species follow the same scale height, and what happens is that as soon as relatively few electrons escape the gravitational pull, a positive space charge is set up, creating a potential Φ_g which prevents further escape. This potential may be computed by MHD theory (Spitzer, 1962, sect. 4.2) or even by means of a variant of eq. (16), but a simple heuristic method given

below also leads to the same result, as long as the energy distributions of ions and electrons coincide (for Φ_g in some more general cases, see Banks and Kockarts [1973], sect. 21.6).

Let $\Omega(z)$ be the gravitational potential at an altitude z and let no additional source of electric field be present. The energy of ionospheric particles is then, for ions

$$W_i = m_i v_i^2/2 + m_i \Omega + e\Phi_g \qquad (77a)$$

and for electrons

$$W_e = m_e v_e^2/2 + m_e \Omega - e\Phi_g \qquad (77b)$$

The density distribution in z of an isolated atmospheric constituent depends entirely on the effective potential to which its particles are subjected. Hence, in order for the ions and electrons to have the same density at any z they must sense the same potential, i.e.

$$m_i \Omega + e\Phi_g = m_e \Omega - e\Phi_g$$

$$= e\chi \qquad (78)$$

From this

$$e\Phi_g = -\Omega(m_i - m_e)/2 \qquad (79)$$

$$e\chi = \Omega(m_i + m_e)/2 \qquad (80)$$

Note that for all practical purposes m_e can be ignored here. The effect of Φ_g is essentially to compensate for half of the weight difference between O^+ ions and electrons, subtracting it from the weight of ions and adding it to that of electrons, so that both species sense the same combined potential $e\chi(z)$. When an external electric potential Φ is added, its effects are added to this, giving for ions

$$W_i = m_i v_i^2/2 + e(\phi+\chi) \qquad (81a)$$

and for electrons

$$W_e = m_e v_e^2/2 - e(\phi-\chi) \qquad (81b)$$

In principle, everything here could be represented in terms of gravity and the total electric potential $\phi'=(\phi+\phi_g)$, with ϕ' derived from quasi-neutrality: this is the course chosen by Chiu and Schulz (1978) and presumably, near s=L their derived E_n resembles the PR field. The notation of (81), however, will be used here, as it is more symmetric and transparent : it suggests that the various densities derived in the preceding section should be modified by the replacement of ϕ by $(\phi+\chi)$ for ions and $(\phi-\chi)$ for electrons, and in many cases this indeed holds.

At low altitudes a simple linear approximation may be used

$$\Omega = m\ g\ z \qquad (82)$$

Since $\gamma(s)$ rather than s is used to indicate position, one would prefer to express Ω as a function of γ. Again, at the level of this model a crude approximation should suffice, since gravity effects are confined to low altitudes: at higher altitudes the externally imposed potential greatly exceeds χ and the exact form of χ (or even its presence) makes only a small difference. If γ is proportional to the inverse cube of the distance, and if altitude zero is assigned to γ_L, then

$$\gamma_L/\gamma = (1 + z/R_E)^3 \qquad (83a)$$

and a useful linear approximation is

$$z/R_E \nu [(\gamma_L/\gamma)-1]/3 \qquad (83b)$$

The escape energy of an O^+ ion can be evaluated from the full inverse square form of Ω and is

$$W(\infty) = m_i g R_E \nu 10.45 \text{ ev} \quad (84)$$

Hence, if (82) is assumed and m_e is neglected

$$e\chi = W(\infty)[(\gamma_L/\gamma)-1]/6 \quad (85)$$

For high altitudes (small γ) this gives values of χ which are far too large. Since (as noted before) the form of χ at these altitudes needs not be very accurate, a simple cutoff approximation will be used, namely

$$e\chi = W(\infty)[(\gamma_L/\gamma)-1]/6 \qquad \gamma > \gamma_L/2 \quad (86a)$$

$$e\chi = W(\infty)/6 = e\chi_o \qquad \gamma < \gamma_L/2 \quad (86b)$$

b. A Naive Model

With gravity and the PR model added, eqs. (64) and (65) are now modified to

$$V_{e1}^2 + (2e/m_e)\chi_o =$$

$$= v_{e1\parallel}^2 + v_{e1\perp}^2 - (2e/m_e)(\Phi - \chi) \quad (87a)$$

$$V_{i1}^2 + (2e/m_i)\chi_o =$$

$$= v_{i1\parallel}^2 + v_{i1\perp}^2 + (2e/m_i)(\Phi + \chi) \quad (87b)$$

with χ_o given by (86b). As before, it is assumed that at s the smallest $v_\parallel$ of either species is zero, belonging to locally mirroring particles. The largest value belongs to particles mirroring at s=L, where $\chi(L)=0$. This gives

$$v_{e1\parallel}^2(\max) = [V_{e1}^2 + (2e/m_e)(\Phi_L+\chi_o)][1-(\gamma/\gamma_L)] -$$

$$- (2e/m_e)[\phi_L - (\phi-\chi)] \qquad (88a)$$

$$v_{i1n}^2(\max) = [V_{i1}^2 - (2e/m_i)(\phi_L-\chi_o)][1-(\gamma/\gamma_L)] +$$

$$+ (2e/m_i)[\phi_L - (\phi+\chi)] \qquad (88b)$$

Comparison to (67) and (69) shows that indeed ϕ has been replaced by $(\phi-\chi)$ or $(\phi+\chi)$ as predicted, but in addition there also exists a dependence on χ_o, because particles starting out at s=0 have ϕ=0 but $\chi=\chi_o$. Since χ drives both species downwards it introduces no special complications and the densities of these species are given by a slight modification of (70) in which (88) is substituted:

$$n_{e1}(\gamma) = 2\,(N_{e1}/V'_{e1})\,v_{e1n}(\max) \qquad (89a)$$

$$n_{i1}(\gamma) = 2\,(N_{i1}/V'_{i1})\,v_{i1n}(\max) \qquad (89b)$$

where

$$(V'_{e1})^2 = V_{e1}^2 + (2e/m_e)\,\chi_o \qquad (90a)$$

$$(V'_{i1})^2 = V_{i1}^2 + (2e/m_i)\,\chi_o \qquad (90b)$$

For electrons from below

$$V_{e2}^2 - (2e/m_e)\phi_L = v_{e2n}^2 + v_{e2\perp}^2 - (2e/m_e)(\phi-\chi) \qquad (91)$$

At any point, the largest v_n belongs (as before) to electrons with $v_{e2\perp}$=0, the smallest to those that mirror locally due to the opposing electric field. This gives relations completely analogous to (74), except that $(\phi-\chi)$ replaces ϕ

$$v_{e2n}^2(\max) = [V_{e2}^2 - (2e/m_e)(\phi_L - (\phi-\chi))]\theta \qquad (92a)$$

$$v_{e2n}^2(\min) = 0 \qquad (92b)$$

No new physical effects exist, since χ and ϕ both have similar effects, tending to drive the ionospheric electrons back. Applying the same criteria to ions gives, in analogy with (71) and (73) and with a θ function added (see below)

$$v_{i2n}^2(\max) = [V_{i2}^2 + (2e/m_i)(\phi_L - (\phi+\chi))]\theta \qquad (93a)$$

$$v_{i2n}^2(\min) = [V_{i2}^2(1-(\gamma/\gamma_L)) + (2e/m_i)(\phi_L - (\phi+\chi))]\theta \qquad (93b)$$

A "naive" model with the above limits on v_n^2 of its four components was analyzed by the methods of the previous sections, and it yielded solutions analogous to those deri[illegible] there, with a voltage jump somewhere in the range where triple solutions to the QN condition exist.

The results are given in Table 2: the overall voltage profiles closely resemble those of Figure 11, the density profile for small values of γ is also very similar (being essentially Perssonian), and the "double layer" is shifted only slightly and is now located at γ=179.96. Unlike the results of Table 1, the profiles of density and voltage now match their boundary values at s=L, but the density distribution is quite different and changes markedly around γ=382. It is instructive to examine the reason for this.

In the potential of (85) or (86), an ionospheric particle with 0.25 ev can rise unassisted to about γ=382. In the present model, it appears, the effects of the external E_n at altitudes below that level are minimal, so that most of the ionospheric density is confined below that γ and only a few ions manage to rise above it. While these ions do produce a double layer transition, it is located in the rarefied region well above γ=382 and can hardly qualify as a boundary between "ionosphere" and "magnetosphere."

However this model, like the one that preceded it, also has a qualitative flaw, although this is not immediately evident. The

problem involves accessibility: although $E_{\parallel}$ tends to accelerate ions upwards, χ tends to drive them back and imposes upon them at low altitudes a barrier which they must first overcome before they can be freely accelerated.

The situation is schematically illustrated in Figure 12. The dashed line represents a continuous solution for $\Phi(s)$ resembling Persson's, the lower line represents the approximation (86) for χ (greatly exaggerated) and the higher solid line is the sum of the two, which constitutes the "effective potential" sensed by ions. This sum peaks at some point γ_c (c for "critical"), at a value of $(\Phi_c+\chi_c)>1$, and this peak will turn back those ionospheric ions which have started out at s=L with sufficiently small values of $v_{i2\parallel}$.

At altitudes below the barrier such ions are automatically excluded by (93). For $\gamma>\gamma_c$, however, the present formulation allows them to reappear and be accelerated, as if they had managed to "tunnel" through the barrier. Alternatively, the solution is the one which would result if above the barrier there exists a population of trapped ions (trapped in the sense of Chiu and Schulz, 1978, end of p. 631), with a distribution function $F_{i2}(W,\mu)$ exactly matching that of ions below the barrier. Physically, however, such a match does not have any special virtues: it would be more appropriate either to derive the trapped population independently, or to assume that it vanishes. That second possibility is explored next.

c. Solutions with a Barrier

(In this subsection, any velocity etc. appearing without an index giving the population to which it applies refers to the (i,2) population of ions originating in the ionosphere.)

Let there exist a barrier peak at γ_c, with potential Φ_c (Fig. 12). Ions originating at s=L will decrease their $v_{\parallel}$ between γ_L and γ_c

and consequently, those of them which were emitted with small values of $v_{\parallel}$ will mirror somewhere in that range (Fig. 13, broken line). The largest value of the parallel emission velocity for which this occurs will be denoted by $v_{\parallel c}$ and belongs to ions that mirror at γ_c (solid line trajectory in Fig. 13): all ions with $v_{\parallel}>v_{\parallel c}$ will pass the barrier, all those with $v_{\parallel}<v_{\parallel c}$ are reflected.

Both groups satisfy

$$V^2 + (2e/m_i)\Phi_L = v_{\parallel}^2 + v_{\perp}^2 + (2e/m_i)(\Phi+\chi) \qquad (94)$$

and for ions mirroring at γ_c this defines a useful constant

$$v_{\perp c}^2 = V^2 + (2e/m_i)[\Phi_L - (\Phi_c+\chi_c)] \qquad (95)$$

At any other γ, those ions that mirror at γ_c satisfy

$$v_{\parallel}^2 = [1-(\gamma/\gamma_c)]v_c^2 + (2e/m_i)[(\Phi_c+\chi_c)-(\Phi+\chi)] \qquad (96)$$

For γ less than γ_c, $v_{\parallel}^2(\min)$ is given by the above expression. The fastest ions are those with $v_{\perp}=0$, and by (94) they satisfy

$$v_{\parallel}^2(\max) = V^2 + (2e/m_i)[\Phi_L-(\Phi+\chi)] \qquad (97)$$

For γ more than γ_c, $v_{\parallel}^2(\max)$ is the same as above, but $v_{\parallel}^2(\min)=0$, because there exist locally mirroring ions throughout the range.

The limits on $v_{\parallel}^2$ for other species remain the same as in the "naive model", and hence it should be possible now to express the densities of all 4 species, evaluate the QN eqilibrium profile $\Phi(s)$ and if (as it turns out) that profile is discontinuous, track down the multiple solutions (Φ_1,Φ_2,Φ_3) and place the transition from Φ_1 to Φ_3 wherever the jump condition is satisfied. Before all these steps can be taken, however, the values of γ_c and Φ_c must be derived, because they are as yet undefined parameters of the system.

One begins the derivation by expressing the various plasma densities, using (89) and (75), with the limits on the parallel velocities derived above, and from them one obtains the net excess density n_{ch} of one kind of charge over the other (eq. 76a). Because the limits on the parallel velocities contain γ, γ_c, ϕ and ϕ_c, all these parameters will affect n_{ch}:

$$n_{ch} = n_{ch}(\gamma,\gamma_c,\phi,\phi_c) \qquad (98)$$

One condition which must certainly hold is that the plasma is quasi-neutral at the point (γ_c,ϕ_c), i.e. if in (98) (γ,ϕ) is set equal to (γ_c,ϕ_c), n_{ch} will vanish.

$$n_{ch}(\gamma_c,\gamma_c,\phi_c,\phi_c) = 0 \qquad (99)$$

This equation involves only 2 variables and if one of them is known, in principle the other one can be obtained. The calculation thus starts with a set of trial values of γ_c, in general near the "gravitational limit" $\gamma \sim 382$ (see comments about Table 2). For each such γ_c, (99) is solved by trial and error: more than one solution may exist, but the search should seek the largest one, in the interval

$$\phi_L < \phi_c+\chi_c < \phi_L+W_{i2}$$

In this range, in general, n_{ch} varied monotonically with ϕ and changed its sign, so that solutions were readily found by iteration. As γ_c increased towards γ_L, ϕ_c tended towards ϕ_L, which agrees with the boundary conditions; of course, the height of the barrier tended at the same time to zero, since by (86) $\chi(L)=0$. When on the other hand γ_c dropped appreciably below 382, $(\phi_c+\chi_c)$ became very close to (ϕ_L+W_{i2}), allowing only a tiny trickle of ionospheric ions to pass and essentially isolating the ionosphere from the magnetosphere, similar to the situation encountered in Table 2.

These solutions correspond to the ϕ_3 branch of earlier models, and a different solution branch ϕ_1, matching conditions at $\gamma=1$, also exists. As before, this makes necessary a discontinuous jump between the two branches, and wherever the transition occurs, the jump condition must be fulfilled. What now causes an added complication is the extra undetermined parameter γ_c: for each choice of γ_c, a different location γ_{DL} exists at which the jump condition is satisfied. Only the choice $\gamma_c=\gamma_{DL}$ (unique in the present case) is appropriate, however, for the following reason.

Supppose $\gamma_{DL}>\gamma_c$. The voltage jump associated with the double layer is relatively large compared to the height of the barrier, so that if the transition occured at an altitude lower than γ_c, along the line AB in Figure 14, then the equivalent potential $(\phi+\chi)$ would reach its largest value at B, and it would never attain the value $(\phi_c+\chi_c)$ derived from (99) for the value γ_c used in our formulas.

On the other hand, it is not possible that $\gamma_{DL}<\gamma_c$, for ϕ_3 rises steadily as γ decreases, leveling off close to $\phi+\chi = \phi_c+W_{i2}$ (this is demonstrated in tables 3 and 4: the minute decline following that leveling-off was not considered to be significant). Thus if γD_L is postulated to occur at higher altitudes, the equivalent potential $(\phi+\chi)$ will continue rising after γ_c is passed, and its maximum occurs not at γ_c but at γ_{DL}. Thus the physical situation is only consistent with $\gamma_c=\gamma_{DL}$.

The iterative search now proceeds as follows. A starting value of γ_c is chosen, the QN condition (99) is solved for it, ϕ_1 and ϕ_3 are found there and a discontinuous transition between these two values is assumed to exist. The parameter Q_{DL} of (58) is now evaluated, and the procedure is repeated for a different choice of q_c. By iteration, the value of γ_c where $Q_{DL}=0$ is approximated as closely as one wishes, and this gives the proper solution for the problem on hand.

The calculation of Tables 1 and 2 (with the same input parameters) was repeated, taking into account the barrier, and the results are given in Table 3 and Figure 15. The double layer has now shifted to γ=386.027, below the "gravity limit" of γ=382. As a result, it is quite pronounced, involving a density change by a factor of about 20 (Figure 15). The voltage drop is only of the order of 10% of the entire range; for completeness, the continuation of ϕ_3 has also been included in Table 3, although it has no special meaning. In Nature, of course, the presence of a "trapped" population above the DL may diminish appreciably the density change associated with it and could conceivably eliminate it altogether.

Finally, a few words about the stability of the equilibrium solutions derived here. If an equilibrium is unstable, there generally exist exist alternative solutions towards which the system can evolve. Here, when all factors are considered, only a unique equilibrium solution remains and it is therefore expected to be stable against changes caused by $E_{\parallel}$.

Of course, $E_{\parallel}$ may also cause local instabilities by energizing one species while decelerating the other. Any realistic evaluation of such velocity-space instabilities, however, requires the use of more realistic distribution functions as inputs: the artificial monoenergetic functions used here are very far from maxwellian and are probably inherently unstable to begin with. At the present level of modeling, velocity space instabilities are ignored, since the primary aim is to obtain the overall properties of $E_{\parallel}$.

6. FIELD ALIGNED CURRENTS

a. The Quasi-Neutral Equilibrium

In all the preceding models field lines were assumed to be closed and complete symmetry existed between negative and positive values of v_n of all species. One consequence of that symmetry was that the net current vanished. If however the conditions are such that the loss cone is filled, a certain asymmetry appears and j_n no longer vanishes.

In the model developed below it will be assumed that field lines are "open", as in subsection 2-d-iii and Figure 3, and we begin by considering conditions on the dusk side, where O^+ ions may be accelerated upwards. Two sources of asymmetry exist: first, the distant source region characterized by $\gamma=1$ is now in the polar cusp, where convection constantly causes new particles to arrive and keeps the loss cone filled. Secondly, all ionospheric ions which manage to rise above the potential barrier of Figure 14 escape and never return. Each of these components carries a net upward current, and it is of interest to evaluate and compare the associated current densities.

Consider first the precipitating component. The maximum values of v_n^2 for magnetospheric electrons and ions which move upwards after having mirrored are given by (88)

$$v_{e1n}^2(\max,up) = [V_{e1}^2 + (2e/m_e)(\phi_L+\chi_o)][1-(\gamma/\gamma_L)] - \\ - (2e/m_e)[\phi_L - (\phi-\chi)] \qquad (88a)$$

$$v_{i1n}^2(\max,up) = [V_{i1}^2 - (2e/m_i)(\phi_L-\chi_o)][1-(\gamma/\gamma_L)] + \\ + (2e/m_i)[\phi_L - (\phi+\chi)] \qquad (88b)$$

However, the largest parallel velocities for such particles moving

earthwards now corresponds to zero pitch angle, i.e. $v_\perp = 0$. By (87)

$$v_{e1n}^2(\max,\text{down}) = V_{e1}^2 + (2e/m_e)[(\phi-\chi) + \chi_o] \qquad (100a)$$

$$v_{i1n}^2(\max,\text{down}) = V_{i1}^2 - (2e/m_i)[(\phi+\chi) - \chi_o] \qquad (100b)$$

With these limits the densities are expressed by a generalization of (89) (note the absence of the factor 2, since the population is no longer bidirectional):

$$n_{e1}(\gamma) = (N_{e1}/V'_{e1})[v_{e1n}(\max,\text{up}) + v_{e1n}(\max,\text{down})] \qquad (101a)$$

$$n_{i1}(\gamma) = (N_{i1}/V'_{i1})[v_{i1n}(\max,\text{up}) + v_{i1n}(\max,\text{down})] \qquad (101b)$$

Among the ionospheric ions, the escaping component is the one which crosses the barrier. Its limiting values of v_n^2 are given by (97) and (96)

$$v_{i2n}^2(\max,\text{esc}) = V_{i2}^2 + (2e/m_i)[\phi_L - (\phi+\chi)] \qquad (97)$$

$$v_{i2n}^2(\min,\text{esc}) = v_{\perp c}^2[1-(\gamma/\gamma_c)] + \\ + (2e/m_i)[(\phi_c+\chi_c) - (\phi+\chi)] \qquad (96)$$

where

$$v_{\perp c}^2 = V_{i2}^2 + (2e/m_i)[\phi_L - (\phi_c+\chi_c)] \qquad (95)$$

For γ smaller than γ_c, thus,

$$n_{i2}(\gamma) = (N_{i2}/V_{i2})[v_{i2n}(\max,\text{esc}) - v_{i2n}(\min,\text{esc})] \qquad (102a)$$

For γ larger than γ_c one must add to this the ion population reflected from the barrier, extending from $v_n=0$ (local mirroring) to $v_{i2n}(\min,\text{esc})$. Because among these added ions each rising particle is matched by one on its way back, the expression for their density has a factor 2 (as in 75b), and when this is added to (102a) the result is

$$n_{i2}(\gamma) = (N_{i2}/V_{i2})[v_{i2n}(max,esc) + v_{i2n}(min,esc)] \quad (102b)$$

$$(\gamma > \gamma_c)$$

The density of ionospheric electrons is as before given by (75a), with the limits (92). These expressions are now used to express plasma densities at the boundaries $\gamma=1$ and $\gamma=\gamma_L$, and from the input conditions there plus the neutrality requirement, constants such as N_{1i} are evaluated. Then, as before, we must find the proper values of γ_c and ϕ_c, by first compiling a tabulation of γ_c and matching each value with the appropriate ϕ_c, then by finding for each γ_c other values of ϕ which satisfy the QN condition, and finally finding iteratively which is the value of γ_c where a transition from ϕ_1 to ϕ_3 satisfies the jump condition. The jump condition is evaluated by using the different densities expressed above, and (102a) rather than (102b) is to be used for the ions from below, because all ions entering the DL from below manage to escape.

A calculation following the above lines was carried out for the same plasma population for which Table 3 and Figure 15 were earlier derived; the corresponding results are given here in Table 4 and in Figure 16. As can be seen the results are qualitatively similar, with the DL shifting only slightly to $\gamma=396.57$. The main differences are now a decrease in the magnitude of the density jump and an approximate doubling of the voltage jump.

b. The Current Density

The current density due to any component is given by

$$j = n\ e\ \langle v \rangle \quad (103)$$

In the general case it is necessary to evaluate $\langle v \rangle$ (or else, j

directly) by integration over the distribution function. Here, however, the calculation is simplified because all distribution functions are boxcars, allowing one to take for n the total density of the particles involved and for <v> the mean of their extreme values of v_n. For instance, for precipitating electrons the density includes those values of v_{i1n} that mirror below γ_L, hence

$$n_{e1}(\text{prec}) = (N_{e1}/V'_{e1})[v_{e1n}(\text{max,down}) - v_{e1n}(\text{max,up})] \qquad (104)$$

with

$$\langle v \rangle = (1/2)\,[v_{e1n}(\text{max,down}) + v_{e1n}(\text{max,up})] \qquad (105)$$

From this, by (88a) and (100b)

$$j_{e1} = e(N_{e1}/2V'_{e1})[v^2_{e1n}(\text{max,down}) - v^2_{e1n}(\text{max,up})]$$

$$= e(N_{e1}/2V'_{e1})(\gamma/\gamma_L)[V^2_{e1} + (2e/m_e)(\Phi_L+\chi_o)] \qquad (106)$$

It follows that j_{e1} does not depend on Φ but is proportional to γ (and thus to B), as is expected from a current confined to a single flux tube. Similarly, for magnetospheric ions (88b) and (100b) give

$$j_{i1} = e(N_{i1}/2V'_{i1})(\gamma/\gamma_L)[V^2_{i1} - (2e/m_i)(\Phi_L-\chi_o)] \qquad (107)$$

If Φ_L is small and both species start with the same initial energies, then by (106) and (107) the currents are very nearly proportional to V_{e1} and V_{i1}, and hence they satisfy the Langmuir condition

$$(j_{e1}/j_{i1}) = (m_i/m_e)^{1/2} \qquad (108)$$

The presence of Φ_L only makes the disparity more pronounced, because it increases j_{e1} while diminishing j_{i1}.

If Φ_L greatly exceeds the initial energy of electrons (ions may then be cut off), one gets

$$j_{e1} \propto e(N_{e1}/2V'_{e1})(\gamma/\gamma_L)(2e/m_e)\,\Phi_L \qquad (109)$$

The current is then proportional to the total voltage drop Φ_L, and the rate at which j_{e1} deposits energy in the ionosphere is proportional to Φ_L^2, in agreement with published results (Knight, 1973; Lyons et al. 1979; Fridman and Lemaire, 1980).

Intuitively this may be interpreted as follows. Because the distribution function of electrons is assumed to be isotropic, j_{e1} is proportional to the solid angle subtended by the loss cone at $\gamma=1$. For electrons, the parallel field magnifies this solid angle, since it accelerates them downwards and causes the loss of some of them which might have have mirrored if no $E_\parallel$ existed; and by (109), for large voltages, this magnification is in direct proportion to Φ_L. For ions, on the other hand, deceleration takes place and the loss cone shrinks; it may even vanish altogether, if $E_\parallel$ is strong enough to cause all ions to be reflected before reaching s=L.

The rising ion current has a similar form, since (102a) resembles (104)

$$j_{i2} = e(N_{i2}/V_{i2})\,[v^2_{i2\parallel}(\max,\mathrm{esc}) - v_i^2(\min,\mathrm{esc})]$$

$$= e(N_{i2}/V_{i2})(\gamma/\gamma_c)\,[V^2_{i2} - (2e/m_i)(\Phi_L - (\Phi_c+\chi_c))] \qquad (110)$$

The magnitude of j_{i2} is controlled by several factors, but overall it is much smaller than j_{i1}. Ignoring the effect of the potentials in (110) leaves

$$e\,N_{i2}\,V_{i2}\,(\gamma/\gamma_c)$$

In the present model, ionospheric particles have 0.25 ev vs. 2 kev

for magnetospheric ions, V_{i2} is 90 times smaller than V_{i1}, and even if N_{i2} exceeds N_{i1} by a factor 25, j_{i2} still comes out several times smaller than j_{i1}, which was already shown to be only a small fraction of j_{e1}. Taking into account ϕ_L only further reduces j_{i2}, and in the model analyzed here it was found (for ϕ_c and γ_c satisfying the jump condition) that

$$j_{e1}/j_{i1} \simeq 1600$$

All this agrees not only with our initial guesses but also with observations which suggest that j_n is carried primarily by electrons and that its order of magnitude agrees with what may be expected from loss cone precipitation. For instance, for N_{e1} of $1cm^{-3}$ and a starting energy of 0.5 kev

$$e\, N_{e1}\, V_{e1}/2 = 1.06\ \mu A/m^2$$

c. Downflowing Currents

The preceding derivations of $(n_{e1}, n_{i1}, n_{e2}, n_{i2})$ only involve the input densities and energies of the various plasma species. If those are left unchanged, the same profiles of ϕ (with the same values of γ_c and ϕ_c) also furnish QN equilibrium solutions if the direction of E_n is reversed.

The current densities, however, change appreciably, because their dependence on $\langle v \rangle$ makes them roughly proportional to the (-1/2) power of the mass of the particles involved. Thus j_{i2} is increased by the Langmuir factor $(m_i/m_e)^{1/2} \simeq 171.4$ (assuming O^+ ions are involved) and similar factors also affect the two current densities from the magnetosphere, the one aided by E_n and the one opposed to it. For the same input conditions as those used in preceding calculations, the results are given in the first column of Table 5, and it will be noted there that the net current still flows outwards from the ionosphere, even though this direction is now opposed to E_n. The reason is that for both polarities of E_n,

$j_{\parallel}$ is dominated by the current j_{e1} due to electrons precipitating into the loss cone: when the voltage is reversed, j_{e1} is reduced threefold, but it still remains large enough to swamp everything else.

The calculations were repeated for voltages of P kV, with P ranging from 1.4 to 2.2. This was accomplished by scaling the variables--all energies (including $W(\infty)$ of eq. 84) were divided by a factor P, and the final current densities were then multiplied by $P^{1/2}$. These results are also given in table 5 and they show that for $P \sim 1.42$, $j_{\parallel} \sim 0$, making 1.42 equal to the "thermoelectric potential" of 2-d-iii. This value is relatively large, because the rather high energy of 2 keV was assumed for the precipitating electrons; future studies will investigate the way it changes with input conditions.

At P=2 (not tabulated) the voltage is just sufficient to stop one species from precipitating, and at P=2.2 only two species contribute, both aiding the flow of current: still, the value of $j_{\parallel}$ flowing downwards is still only a fraction of a $\mu A/m^2$. For larger values of P, solutions could not be obtained: it might be that the situation then resembles that of Table 1, where no solution exists either, because the ionospheric boundary plasma then is not properly "held down." In that case gravity and the PR field supply the require holding force, but it could be that whenever P is large, it manages to overcome that force at all levels and thus prevents an equilibrium from existing. If such a large voltage is applied along a field line, one expects the plasma and its electric field to undergo a time-dependent evolution, ending perhaps in an equilibrium state after a sufficient number of "trapped" particles are produced. This, however, is at present only a conjecture, and requires further investigation.

Even though the quantitative values of $j_{\parallel}$ may be too approximate, qualitatively this result agrees with observations by

Iijima and Potemra (1976, Figs. 1 and 3), by which field-aligned currents on the dawn side and on the dusk side of the polar caps have approximately equal magnitudes. If one assumes that these currents are carried mainly by electrons, the magnitude on the dusk side fits quite well the loss-cone precipitation of electrons, but without a calculation similar to the one performed here, it is not immediately evident why a similar current density should exist on the dawn side. On the contrary, it might be argued that even a narrow strip of the ionosphere (e.g. one 10 km wide, as proposed by Knight, 1973, before accurate observations became available) can easily supply enough electrons to carry Birkeland current sheets of sufficient intensity.

The present results suggest that the outflow of such electrons is greatly hampered by the Pannekoek-Rosseland field. Even though the total voltage drop associated with this field is small, a relatively large external voltage must be applied before it is overcome, because most of such a voltage is distributed at higher altitudes, to insure quasi-neutrality, and only a small part remains available lower down, where the PR effect is most pronounced. In the present model, most of this remainder is "used up" in maintaining the DL, so that even at 2.2 kV the PR effect still throttles $j_{\parallel}$ to a considerable extent.

In addition to the above role, $E_{\parallel}$ is also required on the dawn side the polar cap to stem the precipitation of electrons, which opposes the flow of $j_{\parallel}$ fed by external sources. Future studies should provide a more complete modeling of the behavior of this interesting region.

7. SUMMARY

A one-dimensional model of $E_{\parallel}$ has been developed in which field aligned voltage drops are maintained by a quasi-neutral plasma equilibrium. The model assumes two monoenergetic isotropic sources of plasma, a hot dilute magnetospheric one and a cold dense one in the ionosphere.

All equilibria derived here required an abrupt discontinuity embedded in them, a discontinuity in which quasi-neutrality did not hold. A model was therefore derived for the "double layer" discontinuity which arises in such cases, and the "jump condition" (57) which must be satisfied was expressed. It turned out that the discontinuous quasi-neutral solutions were not in general unique, but that among the range of such profiles, one solution could generally be found (Figure 10) for which the jump condition held.

Even then the simplest solutions (Table 1) were not consistent with ionospheric boundary conditions, until gravity was taken into account (in an approximation valid for low altitudes), together with the Pannekoek-Rosseland electric field which accompanies it. Initially, questions of accessibility were ignored and quasi-neutral equilibria were constructed (Table 2) with discontinuous voltage profiles very similar to those obtained before. However, such models are inaccurate, since they required either "tunneling" or a rather artificial "trapped" population.

A more consistent calculation was then undertaken, including a potential barrier which hindered the escape of ionospheric ions; this involved one additional parameter, the location γ_c of the barrier (from this its potential Φ_c was derived using charge neutrality). Here, too, quasi-neutral equilibrium dictated a discontinuous voltage jump, and plausible arguments were given to show that this occurred at γ_c itself. Model calculations in which this barrier was taken into account gave double layers in which the voltage changed only moderately but densities underwent a

marked change (Table 3, Figure 15).

Finally, a current flow was included in the model (Table 4), contributed in part by precipitating magnetospheric particles and in part by escaping ionospheric ones. In regions of upward flowing $j_{\parallel}$, this current was found to be dominated by precipitating electrons (Table 5), to be approximately proportional to the accelerating voltage (or more accurately, to the ratio by which the energy of electrons was increased) and its density was of the order of 1 $\mu A/m^2$. The profiles of density (Figure 16) and of voltage were qualitatively similar to those obtained in the preceding case.

For $E_{\parallel}$ directed towards the Earth the situation was more complicated (Table 5) and for small voltages $j_{\parallel}$ actually opposed $E_{\parallel}$, since it was still dominated by the contribution of loss-cone electrons (in common with currents having upward $E_{\parallel}$). Assuming a distant population of 2 keV electrons, a voltage drop of 1.42 kV was required before $j_{\parallel}$ vanished (yielding an approximate "thermoelectric potential" for equilibrium with $j_{\parallel}=0$ under the given conditions). At 2.2 kV, the current was directed upwards and its density reached a fraction of a $\mu A/m^2$ (though for 3 kV solutions no longer could be found), in rough agreement with observations by which $j_{\parallel}$ is limited to the order of 1 $\mu A/m^2$ for both upflowing and downflowing currents.

While the models developed here are quite rudimentary, they seem to indicate that quasi-neutral equilibria can provide a physically plausible mechanism for maintaining $E_{\parallel}$ and $j_{\parallel}$ in the polar magnetosphere, and in particular in the "region 1" current sheets (Figure 3). "Double layer" type discontinuities occured in all the solutions: whether they persist when more realistic distribution functions and "trapped" particles are included, and whether they are related to the abrupt structures observed aboard S3-3 (Mozer et al., 1977) is left for future investigations to decide. As an incidental byproduct, it is noted here that a net

current flow is not essential for the existence of double layers, and that current-free parallel electric fields may play a role in decoupling distant magnetospheric motions from the ionosphere.

8. OUTLOOK

The present effort suggests three immediate extensions. First, the effects of varying the input parameters should be studied. These include the density and mean energy of the bounding plasmas and the total voltage drop Φ_L; in addition, the effect of a "trapped" population may also be investigated and the reason for the lack of solutions at $\Phi_L > 2.2$kV should be traced.

Secondly, the monoenergetic distributions may be replaced by proper maxwellians, similar to those used by Chiu and Schulz (1978) and by Chiu and Cornwall (1980), but making use of the experience gained here concerning uniqueness and accessibility. Through the use of a maxwellian ionospheric population, it might be possible to construct a model in which a quasi-neutral plasma with $E_n \neq 0$ blends smoothly with an exponential ionosphere, without postulating any ad-hoc "boundary density" at s=L. Something of this sort is already evident in Table 2, but when voltage barriers are included the situation seems to be more complicated.

Finally, one might postulate mechanisms for particle scattering and loss which would support a stable trapped population, and this is expected to modify the voltage profiles to a considerable degree; existing theories of wave-plasma interactions developed for models of j_n in the magnetosphere may be utilized to provide such mechanisms. Ultimately, of course, the consistency of all such theories must be checked against observed particle distributions. In principle, particle data (pitch angles and energies) from two points along the same field line may be able to provide such a check, and it is hoped that the forthcoming Dynamics Explorer mission will indeed provide such data.

Models of this type can be expected to reproduce many of the properties of $E_{\parallel}$ associated with "region 1" current sheets, similar to those in Figure 3. Additional problems arise, however, when such models are applied to "region 2" currents created by "charge separation" (2-d-iv), and this study will conclude with speculations about $E_{\parallel}$ in such cases.

Whenever the convection of electrons produces regions of negative space charge (in general, in the early morning sector and near midnight), the dissipation of such charge is governed by (106), or approximately by (109); while those relations were derived for a rather specific model, other and more elaborate models lead to similar results (Lyons et al., 1979; Fridman and Lemaire, 1980). The point to note is that the current density which can be handled by this mechanism is quite limited: if 1 kev electrons are convected earthwards and a parallel drop Φ_L=20 kV is produced by their space charge, the solid angle covered by their loss cone is increased 20-fold, but because that cone is initially very small (order of 1^o) the loss rate will always be rather modest and, unless scattering is rapid, particles with pitch angles of 10^o or more cannot be easily precipitated.

In contrast, the rate at which free space charge is produced depends only on magnetospheric conditions: what happens, then, when the production rate outstrips the removal rate? The value of Φ_L= 20 kV is already an appreciable fraction of the total voltage drop associated with the convective electric field, and cannot increase much more: indeed, auroral energy spectra often display a sharp cutoff at 10-15 keV (e.g. Evans et al., 1974; Maynard et al., 1977, Figs. 5-6; Bryant et al., 1978), suggesting that Φ_L peaks in this range. Thus it does not appear that $j_{\parallel}$ can be raised by increasing its driving voltage. Neutralization of the negative charge by ionospheric O^+ ions is delayed by their low mobility and requires 2-3 minutes, which may be too slow.

The remaining alternative is that negative charge does indeed

accumulate and that it creates local electric perturbations which steer away convecting electrons to other regions of space. Such charging has been studied by Hallinan (1976), who concluded that it would manifest itself in counterclockwise spiral structures, and those have been observed (Untiedt et al., 1978, p. 51). It may further be speculated that the rapid variability of the aurora could represent a constant shifting of its source region in the equatorial plane, away from field lines which have accumulated an excess of negative space charge.

A second (and perhaps related) problem involves the large abundances of O^+ observed in the ring current (Balsiger et al., 1980), often reaching 20-30% and even more. Supppose that all of $E_{\parallel}$ on field lines threading the ring current is due to charge separation between electrons and ions (presumed to be mostly protons), convected earthwards from the tail. Then for each separated proton there exists one separated electron, and if none of the electrons is precipitated and each of them draws upwards one O^+ ion, the ring current will ultimately contain equal numbers of protons and O^+ ions. In fact, unequal losses due to charge exchange with hydrogen can even cause O^+ to predominate. However, Table 5 suggests that electron precipitation greatly exceeds any upward flow of O^+.

A possible explanation is that scattering of electrons into the loss cone occurs on a time scale much longer than the 2-3 minutes required for O^+ ions to arrive at the region of unbalanced space charge. Thus after the local density of space charge has saturated (in the way described earlier) the population of loss cone electrons quickly becomes depleted, after which the electron current of (106) is greatly diminished, while the ion current of (110) persists for a long time. If this mechanism indeed occurs, one would expect a far greater variability in the intensity of the precipitating electron beam than in that of the O^+ beam associated with it.

In addition, it now appears (Horwitz, 1980; Gorney et al., 1981) that the acceleration of "conic" distribution of O^+ ions by wave-particle interactions constitute an important source of O^+ in the ring current, in addition to the "beams" discussed here. If this indeed proves to be the dominant source, then the discrepancy noted above is avoided.

Acknowledgments: I am grateful to my colleagues Tom Birmingham, Larry Lyons and Jack Scudder who diligently reviewed the original draft of this work and who provided many valuable suggestions, new insights, corrections and additions. In addition, I thank Jim Drake for bringing to my attention the relationship between tandem mirror confinement of fusion plasmas and quasi-neutral electric fields.

REFERENCES

Alfven, H. and C.-G. Fälthammar, Cosmical Electrodynamics, Oxford University Press, Oxford, England, 2nd ed. 1963.

Balsiger, H., P. Eberhardt, J. Geiss and D.T. Young, Magnetic storm injection of 0.9 to 16 keV/e solar and terrestrial ions into the high-altitude magnetosphere, J. Geophys. Res., 85, 1645-1662, 1980.

Banks, P.M. and T.E. Holzer, Features of plasma transport in the upper atmosphere, J. Geophys. Res., 74, 6304-6316, 1969a.

Banks, P.M. and T.E. Holzer, High-latitude plasma transport: the polar wind, J. Geophys. Res., 74, 6317-6332, 1969b.

Banks, P.M. and G. Kockarts, Aeronomy, Academic Press, 1973.

Bernstein, I.B., J.M. Greene and M.D. Kruskal, Exact nonlinear plasma oscillations, Phys. Rev.,108,546-550, 1957

Block, L.P., Potential double layers in the ionosphere, Cosmic Electrodynamics, 3, 349-376, 1972.

Block, L.P., A double layer review, Astrophys. Space Sci., 55, 59-83, 1978.

Bohm, D., Minimum ionic kinetic energy for a stable sheath, Chapt. 3 in The Characteristics of Electrical Discharges in Magnetic Fields, A. Guthrie and R.K. Wakerling, editors, McGraw Hill, 1949.

Bryant, D.A., D.S. Hall and D.R. Lepine, Electron acceleration in an array of auroral arcs, Planet. Space Sci., 26, 81-92, 1978.

Carlqvist, P., Some theoretical aspects of electrostatic

double layers, p.83-108 in Wave Instabilities in Space Plasmas, P.J. Palmadesso and K. Papadopoulos, eds., D. Reidel, 1979.

Chiu, Y.T. and M. Schulz, Self-consistent particleand parallel electrostatic field distributions in the magnetospheric-ionospheric auroral region, J. Geophys. Res., 83, 629-642, 1978.

Chiu, Y.T., M. Schulz and J.M. Cornwall, Auroral magneto-sphere-ionosphere coupling: a brief topical review, pp 494-512 in vol. 2 of Solar Terrestrial Predictions Proceedings, ed. by R.F. Donnelly, NOAA, Boulder, Colo., 1980.

Chiu, Y.T. and J.M. Cornwall, Electrostatic model of a quiet auroral arc, J. Geophys. Res., 85, 543-556, 1980.

Coensgen, F.H., et al., Electrostatic plasma-confinement experiments in a tandem mirror system, Phys. Rev. Let., 44, 1132-1135, 1980.

Cohen, B.I. (editor), Status of Mirror Fusion Research 1980, Report UCAR-10049-80-Rev.1, Lawrence Livermore National Laboratory, 1980.

Coroniti, F.V., L.A. Frank, R.P. Lepping, F.L. Scarf and K.L. Ackerson, Plasma flow pulsations in the Earth's magnetic tail, J. Geophys. Res., 83, 2162-2168, 1978.

Courant, R. and D. Hilbert, Methods of Mathematical Physics, Vol. 1, Interscience Publishers, Inc., 1953.

Dimov, G.I., V.V. Zakaidakov and M.E. Kishinevsky, Thermonuclear confinement system with twin mirror systems, Sov.J. Plasma Phys. (tranlation) 2, 326-333, 1976 (Fiz. Plazmy, 2, 597-610, 1976).

Evans, D.S., Precipitating electron fluxes formed by a

magnetic field aligned potential difference, J. Geophys. Res., 79, 2853-2858, 1974.

Fowler, T.K. and B.G. Logan, The tandem mirror reactor, Comment. Plasma Phys. Con. Fus., 2, 167-172, 1977.

Fridman, M. and J. Lemaire, Relationship between auroral electrons fluxes and field aligned electric potential difference, J. Geophys. Res., 85, 664-670, 1980.

Ghielmetti, A.G., R.G. Johnson, R.D. Sharp and E.G. Shelley, The latitudinal, diurnal and altitudinal distributions of upward flowing energetic ions of ionospheric origin, Geophys. Res. Let., 5, 59-62, 1978.

Goertz, C.K., Double layers and electrostatic shocks in space, Rev. Geophys. Space Phys., 17, 418-426, 1979.

Gurney, D.J., A. Clarke, D.R. Croley, J.F. Fennell, J.M. Luhmann and P.F. Mizera, The distribution of ion beams and conics below 8000 km, J. Geophys. Res., 86, 83-89, 1981.

Hallinan, T.J., Auroral Spirals: 2. Theory, J. Geophys. Res., 81, 3959-3965, 1976.

Hasan, S.S. and D. Ter Haar, The Alfven-Carlquist double-layer theory of solar flares, Astrophys Space Sci., 56, 89-107, 1978.

Horwitz, J.L., Conical distributions of low-energy ion fluxes at synchronous orbit, J. Geophys. Res., 85, 2057-2064, 1980.

Hultqvist, B., On the interaction between the magnetosphere and the ionosphere, Proc. of the STP Symposium, Leningrad, May 1970.

Hultqvist, B., On the production of a magnetic-field-aligned electric field by the interaction between the hot magnetospheric

plasma and the cold ionosphere, Planet. Space Sci., 19, 749-759, 1971.

Iijima, T. and T. Potemra, The amplitude distribution of field aligned currents at northern high latitudes observed by Triad, J. Geophys. Res., 81, 2165-2174, 1976.

Kan, J.R., Energization of auroral electrons by electrostatic shock waves, J. Geophys. Res., 80, 2089-2095, 1975.

Kan, J.R., Comment on 'Double layers and electrostatic shocks in space" by C.K. Goertz, Rev. Geophys. Space Phys., 18, 338, 1980.

Kan, J.R. and L.C. Lee, On the auroral double layer criterion, J. Geophys. Res., 85, 788-790, 1980a.

Kan, J.R. and L.C. Lee, Double layer criterion on the altitude of the auroral acceleration region, Geophys. Res. Let., 7, 429-432, 1980b.

Knight, S., Parallel electric fields, Planet. Space Sci., 21, 741-750, 1973.

Lemaire, J. and M. Scherer, Ionosphere-plasmasheet field-aligned currents and parallel electric fields, Planet. Space Sci., 22, 1485-1490, 1974.

Lemaire, J. and M. Scherer, Field aligned distribution of plasma mantle and ionospheric plasma, J. Atmos. Terrestr. Phys., 40, 337-342, 1978.

Lennartsson, W., On the magnetic mirroring as the basic cause of parallel electric fields, J. Geophys. Res., 81, 5583-5586, 1976.

Lennartsson, W., On the role of magnetic miroring in the auroral phenomena, Astrophys. Space Sci., 51, 461, 1977.

Lennartsson, W., On the parallel electric field associated with magnetic mirroring of auroral electrons--some basic physical properties, Technical Report TRITA-EPP-78-08, The Royal Inst. of Technology, S-10044 Stockholm 70, Sweden, 1978.

Lennartsson, W., On the consequences of the interaction between the auroral plasma and the geomagnetic field, Planet. Space Sci., 28, 135-147, 1980.

Levine, J.S. and F.W. Crawford, A fluid description of plasma double-layers, J. Plasma Phys., 23, 223-247, 1980.

Lyons, L.R., Generation of large-scale regions of auroral currents, electric potentials, and precipitation by the divergence of the convection electric field, J. Geophys. Res., 85, 17-24, 1980a.

Lyons, L.R., Discrete aurora as the direct result of an inferred, high-altitude generating potential distribution, J. Geophys. Res., 86, 1-8, 1981.

Lyons, L.R., D.S. Evans and R. Lundin, An observed relation between magnetic field aligned electric fields and downward electron fluxes in the vicinity of auroral forms, J. Geophys. Res., 84, 457-461, 1979.

Maeda, K. and S. Kato, Electrodynamics of the ionosphere, Space Sci. Rev. 5, 57-79, 1966.

Maynard, N.C., D.S. Evans, B. Maehlum and A. Egeland, Auroral vector electric field and particle comparisons, 1. Premidnight convection topology, J. Geophys. Res., 82, 2227-2234, 1977.

Mozer, F.S., C.W. Carlson, M.K. Hudson, R.B. Torbert, B. Parady, J. Yatteau and M.C. Kelley, Observations of paired electrostatic shocks in the polar magnetosphere, Phys. Rev. Let., 38, 292-295, 1977.

Mozer, F.S., C.A. Cattell, M. Temerin, R.B. Torbert, S. Von Glinski, M. Woldorff and J. Wygant, The dc and ac electric field, plasma density, plasma temperature, and field-aligned current experiments on the S3-3 satellite, J. Geophys. Res., 84, 5875-5884, 1979.

Mozer, F.S. and R.B. Torbert, An average parallel electric field deduced from the latitude and altitude variations of the perpendicular electric field below 8000 kilometers, Geophys. Res. Let., 7, 219-221, 1980.

Pannekoek, A., Ionization in stellar atmospheres, Bull. Astron. Inst. Neth., 1, 107-118, 1922.

Papadopoulos, K., A review of anomalous resistivity for the ionosphere, Rev. Geophys. Space Phys., 15, 113-127, 1977.

Perkins, F.W. and Y.C. Sun, Double layers without current, Phys. Rev. Let., 46, 115-118, 1981.

Persson, H., Electric field along a magnetic line of force in a low-density plasma, Phys. Fluids, 6, 1756-1759, 1963.

Persson, H.,Electric field parallel to the magnetic field in a low density plasma, Phys. Fluids, 9, 1090-1098, 1966.

Rosseland, S., Electrical state of a star, Monthly Notices of the R.A.S., 84, 720-728, 1924.

Schield, M.A., J.W. Freeman and A.J. Dessler, A source for field aligned currents at auroral latitudes, J. Geophys. Res., 74,

247-256, 1969.

Schwarzschild, B.M., Tandem mirror sucess leads to expanded MFTF (report), Physics Today, 33, 17-19, October 1980.

Spitzer, L., Jr., Physics of Fully Ionized Gases, Interscience Publishers (John Wiley and Sons), 2nd ed., 1962.

Stenzel, R.L., M. Ooyama and Y. Nakamura, V-shaped double layers formed by ion beam reflection, Phys. Rev. Let., 45, 1498-1501, 1980.

Stern, D.P., The electric field and global electrodynamics of the magnetosphere, Rev. Geophys. Space Phys., 17, 626-640, 1979.

Stern, D.P., Large-scale electric fields in the Earth's magnetosphere, Rev. Geophys. Space Phys., 15, 156-194, 1977.

Torbert, R.B. and C.W. Carlson, Evidence for parallel electric field particle acceleration in the dayside auroral oval, J. Geophys. Res., 85, 2909-2914, 1980.

Untiedt, J., et al., Observations of the initial development of an auroral and magnetic substorm at magnetic midnight, J. of Geophysics, 45, 41-65, 1978.

Whipple, E.C., Jr., The signature of parallel electric fields in a collisionless plasma, J. Geophys. Res., 82, 1525-1531, 1977.

Wolf, R.A., Ionosphere-magnetosphere coupling, Space Sci. Rev., 17, 537-562, 1975.

Zmuda, A.J. and J.C. Armstrong, The diurnal flow pattern of field aligned currents, J. Geophys. Res., 79, 4611-4619, 1974.

CAPTIONS TO FIGURES

Figure 1 -- Schematic representation of the effect of E_n in a homogeneous magnetic field (1a) and in a geomagnetic mirror geometry (1b).

Figure 2 -- The geometry assumed in Persson's calculation and the notation used.

Figure 3 -- Schematic view of a circuit producing field aligned currents along open field lines linking the solar wind to the polar ionosphere.

Figure 4 -- Collision-free plasma in a homogeneous magnetic field, subject to a fixed potential drop Φ_{AB}. Under such conditions the entire drop tends to become concentrated in a narrow sheath.

Figure 5 -- The voltage profile across a double layer and the different particle populations which enter it.

Figure 6 -- Schematic view of a magnetic flux tube (drawn without its curvature) subject to a parallel voltage drop Φ_L, and with the various particle populations which enter it.

Figure 7 -- Schematic view of the net charge excess $n_{ch}(\Phi,\gamma)$ as a function of Φ, for a fixed small value of γ. Both axes are unevenly divided in order to bring out the qualitative properties of the curve.

Figure 8 -- Similar to Figure 7, showing the existence of 3 solutions (Φ_1,Φ_2,Φ_3) for intermediate values of γ.

Figure 9 -- Similar to Figure 7, showing conditions for values of γ near γ_L, when again only a unique solution exists.

Figure 10 -- Similar to Figure 7, at the value of γ where the double layer condition is satisfied. The two shaded areas are equal to each other.

Figure 11 -- The 3 solutions (ϕ_1, ϕ_2, ϕ_3) to the quasi-neutrality condition, plotted against γ for the simple gravity-free model (as noted in the text, this solution does not fulfil all requirements). The y coordinate is proportional to $-\log(\phi_L - \phi)$ and is labeled in fractions of ϕ_L. The input conditions are ϕ_L=1000 V, $W_{i1}=W_{e1}$=2 keV, $W_{i2}=W_{e2}$=0.25 ev, $n_{i1}=n_{i2}$=1 cm^{-3}, $N_{i2}=N_{e2}$=25 cm^{-3}, γ_L=436.

Figure 12 -- Schematic representation of the potential sensed by ions, being the sum of an externally imposed electric potential ϕ (drawn here without any abrupt discontinuities and the combined potential χ contributed by gravity and by the PR field.

Figure 13 -- The motion of ionospheric ions in a geomagnetic flux tube (drawn without its curvature) under the influence of the potential of Figure 12. The dashed line represents the trajectory of an ion reflected by the potential barrier, while the solid trajectory belongs to an ion which mirrors at γ_c and which is therefore on the threshold of escaping.

Figure 14 -- The assumed curve of the effective potential ($\phi+\chi$) sensed by ions, near $\gamma=\gamma_c$. If the abrupt transition occured along AB, then ($\phi_c+\chi_c$) would not be the largest value of the effective potential in the range.

Figure 15 -- The density profile of a plasma similar to that of Figure 11 and Table 1, but incorporating the effects of gravity and of a potential barrier.

Figure 16 -- The density profile obtained for the case illustrated in Figure 15, if one allows free escape of ionospheric ions and if the loss-cone population of magnetospheric particles is constantly replenished to the same level as the one existing outside the loss cone.

Table 1

γ	ϕ_1	ϕ_2	ϕ_3	n_1	n_3
1	0.0			1.0	
2	0.0032			0.9991	
5	0.0128			0.9963	
10	0.0289			0.9917	
20	0.0611			0.9824	
30	0.0933	0.9995	0.999 505 0995	0.9730	1.1838
50	0.1583	0.9981	0.999 750 1166	0.9541	1.6942
80	0.2568	0.9942	0.999 750 5687	0.9253	2.3009
120	0.3914	0.9844	0.999 751 7392	0.8863	3.1296
160	0.5333	0.9655	0.999 753 6199	0.8477	3.9844
183.91	0.6263	0.9452	0.999 755 1175	0.8263	4.5097
200	0.6979	0.9220	0.999 756 2961	0.8143	4.8869
240			0.999 759 8803		5.7925
280			0.999 764 5267		6.7601
320			0.999 770 4556		7.7839
360			0.999 778 0053		8.8795
400			0.999 787 7627		10.0687
420			0.999 793 8380		10.7036
435			0.999 799 416		11.1728
435.99			0.999 800 110		11.1926

The three solutions for the voltage at which quasi-neutral equilibrium may exist, and corresponding plasma densities, for a gravity-free model with both magnetospheric and ionospheric sources (see text: this model does not satisfy all requirements). Spaces left blank mean that a particular solution does not exist.

Table 2

γ	Φ_1	Φ_3	n_1	n_3
2	0.0032		0.9991	
5	0.0128	0.998 450 9316	0.9963	1.2195
10	0.0289	0.998 390 6543	0.9917	1.2124
20	0.0611	0.998 145 6204	0.9824	1.1980
30	0.0934	0.997 723 8220	0.9730	1.1834
50	0.1583	0.996 289 4530	0.9540	1.1535
80	0.2569	0.992 364 4393	0.9252	1.1068
120	0.3916	0.998 471 6220	0.8862	1.0440
160	0.5337	0.998 471 6319	0.8477	0.9756
179.96	0.6107	0.998 471 6369	0.8296	0.9395
200	0.6989	0.998 471 6418	0.8144	0.9098
240		0.998 797 6733		0.8220
280		0.999 259 1944		0.7335
320		0.999 605 3376		0.6326
360		0.999 874 5623		0.5122
380		0.999 987 9209		0.4396
382		0.999 998 6039		0.4317
383		0.999 999 7733		3.4650
385		0.999 999 5730		6.3369
400		0.999 999 1043		15.2738
415		0.999 999 0876		20.2130
430		0.999 999 4214		23.8403
435		0.999 999 7532		24.8411
436		1.0		25.

Similar to Table 1, with gravity incorporated but accessibility considerations ignored. In this table and the ones that follow the Φ_2 branch is omitted, since it is never used. Note how the "ionospheric" and "magnetospheric" regimes have a relatively well-defined boundary at γ=382, differing from the double layer at γ = 179.96

Table 3

γ	$\Phi_1+\chi_1$	$\Phi_3+\chi_3$	n_1	n_3
436		1.0		25.0
435		1.000 003 841		24.841
430		1.000 024 235		23.840
425		1.000 045 281		22.735
420		1.000 066 895		21.531
415		1.000 089 074		20.213
410		1.000 111 830		18.758
405		1.000 135 182		17.131
400		1.000 159 152		15.274
395		1.000 183 768		13.085
390		1.000 209 071		10.345
386.027	0.9247	1.000 229 714	0.3669	7.358
380	0.9088	1.000 249 986	0.3840	0.4406
370	0.8335	1.000 249 983	0.4113	0.4773
350	0.8344	1.000 249 979	0.4621	0.5448
300	0.7141	1.000 249 966	0.5706	0.6849
250	0.5950		0.6618	
200	0.4761		0.7420	
150	0.3568		0.8145	
100	0.2375		0.8811	
50	0.1185		0.9430	
1	0.0017 783 = χ_o		1.0	

Similar to the preceding table, but taking into account the accessibility restrictions imposed by gravity and by the PR potential. All rising ions ultimately return and the loss cone is empty of magnetospheric particles, hence $j_n=0$.

Table 4

r	$\phi_1+\chi_1$	$\phi_3+\chi_3$	n_1	n_3
435		1.000 003 383		25.1450
430		1.000 020 892		23.9605
425		1.000 038 820		22.6597
420		1.000 057 108		21.2292
415		1.000 075 706		19.6373
410		1.000 094 513		17.8301
405		1.000 113 264		15.7057
400		1.000 131 017		13.0025
396.57	0.8058	1.000 139 333	0.6910	10.1478
390	0.7795	1.000 188 750	0.6996	7.6780
370	0.7092	1.000 249 848	0.7254	0.8515
350	0.6485	1.000 249 835	0.7492	0.8852
300	0.5208		0.8007	
250	0.4131		0.8437	
200	0.3175		0.8813	
150	0.2299		0.9151	
100	0.1487		0.9458	
50	0.0725		0.9741	
1	0.0017783 = χ_o			

Similar to Table 3, but now rising ions are allowed to escape and the loss cone is filled with magnetospheric particles, both effects contributing to a non-zero j_n.

Table 5

voltage kV	1	1.4	1.42	1.8	1.9	2.2
γ_c	396.57	404.4	404.8	412.8	415.5	427.8
$(\Phi_3+\chi-1).10^6$	139.333	46.692	62.2074	27.471	20.507	3.701
$(\Phi_1+\chi)$	0.8058	0.8359	0.8379	0.8217	0.8038	0.7769
n_3	10.1478	13.154	13.304	16.291	17.300	21.985
n_1	0.6910	0.6758	0.6746	0.6603	0.6649	0.6819
Upflowing j_n						
j_{e1}	364.1	412.7	415.1	461.3	473.4	509.9
j_{i1}	2.83	1.70	1.65	0.57	0.29	0
j_{i2}	0.224	0.349	0.355	0.481	0.499	0.634
Downflowing j_n						
j_{i1}	8.50	9.63	9.69	10.76	11.05	11.90
j_{e1}	121.43	72.93	70.51	24.45	12.33	0
j_{e2}	38.42	59.76	60.85	82.55	89.71	119.46

Values of γ_c for various voltage drops in kilovolts, together with the potentials Φ_1 and $\Phi_3=\Phi_c$ and the corresponding densities bounding the double layer (for the sake of brevity, $\Phi_c+\chi$ is encoded: its value in the first column, for instance, is 1.000 139 333). For each voltage, the 3 components of the current density at γ_L are given, in relative units. Apart from the total voltage drops conditions resemble those assumed in the preceding tables.

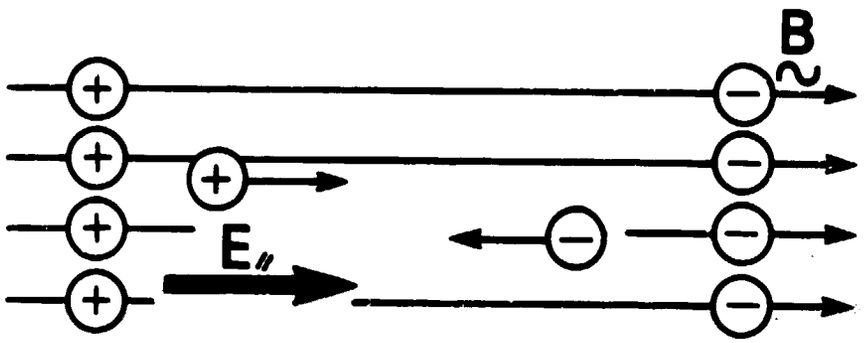

Figure 1a

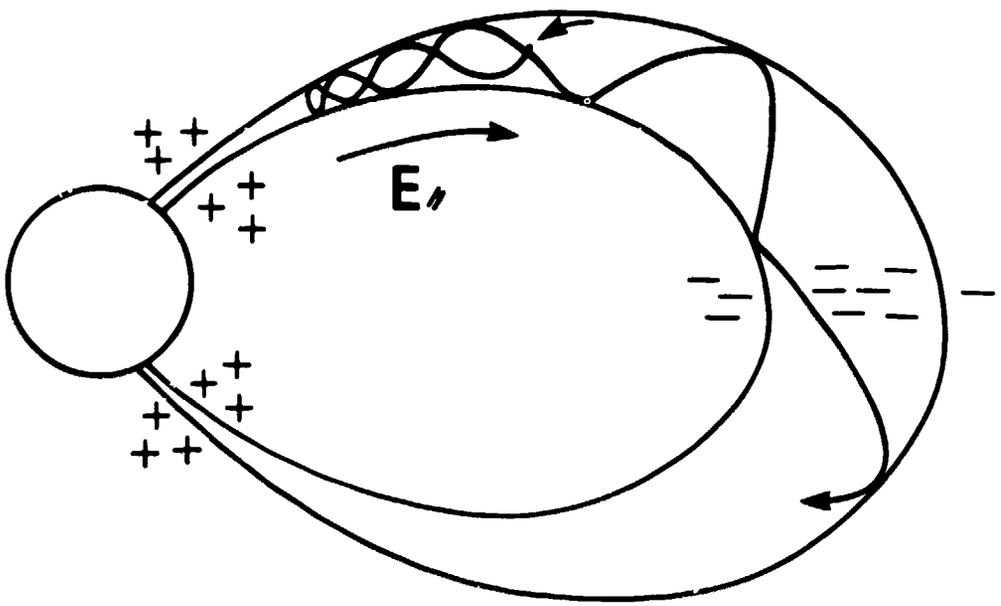

Figure 1b

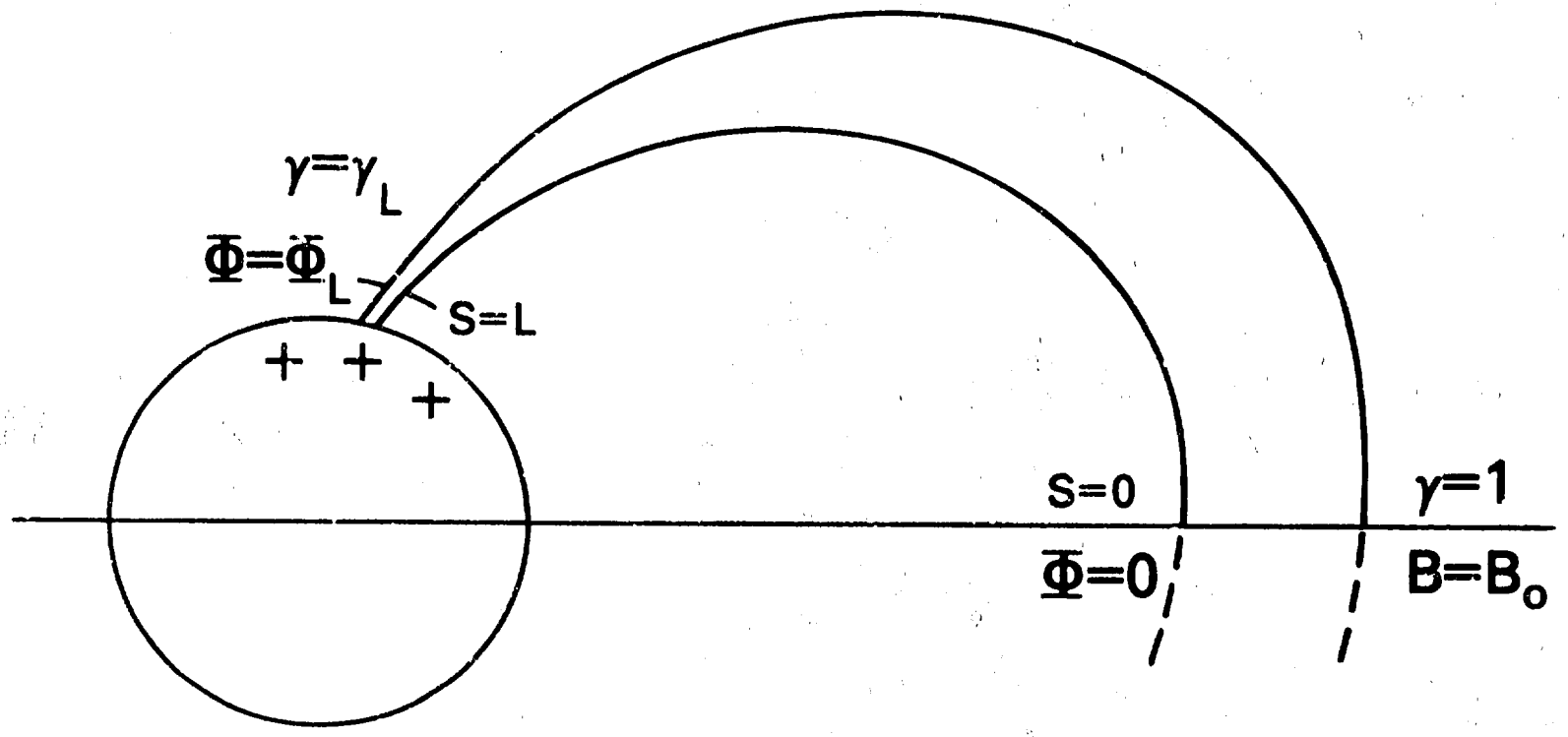

Figure 2

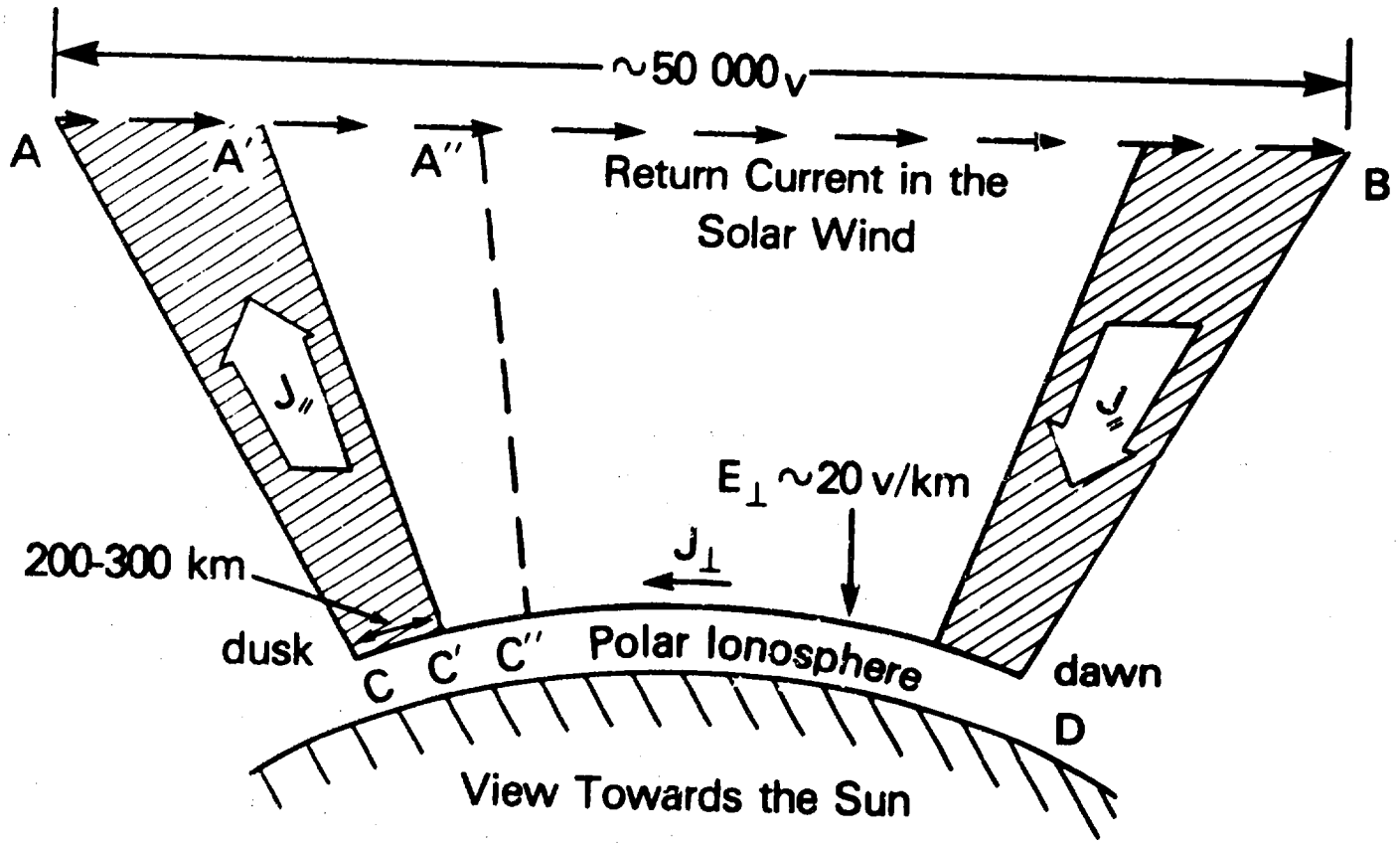
~50 000 v
A
A'
A''
Return Current in the
Solar Wind
B
J//
J⊥
E⊥ ~20 v/km
200-300 km
J⊥
dusk
C C' C''
Polar Ionosphere
dawn
D
View Towards the Sun

Figure 3

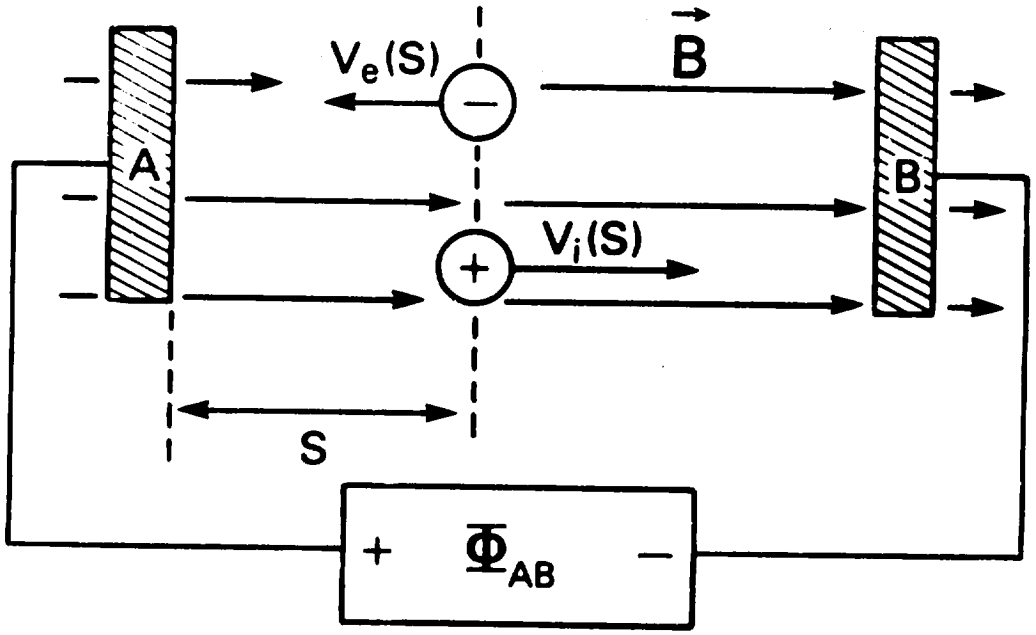

Figure 4

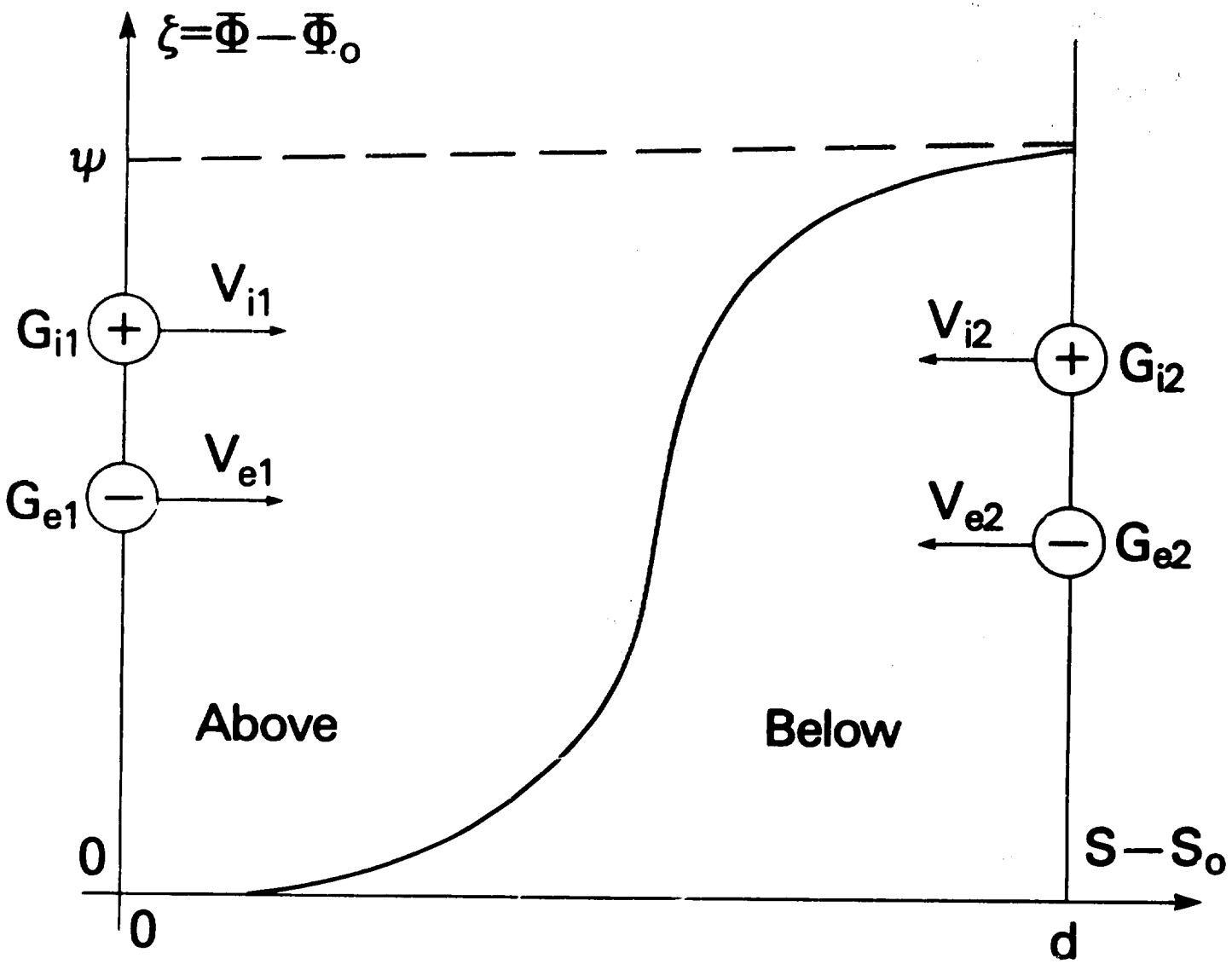

Figure 5

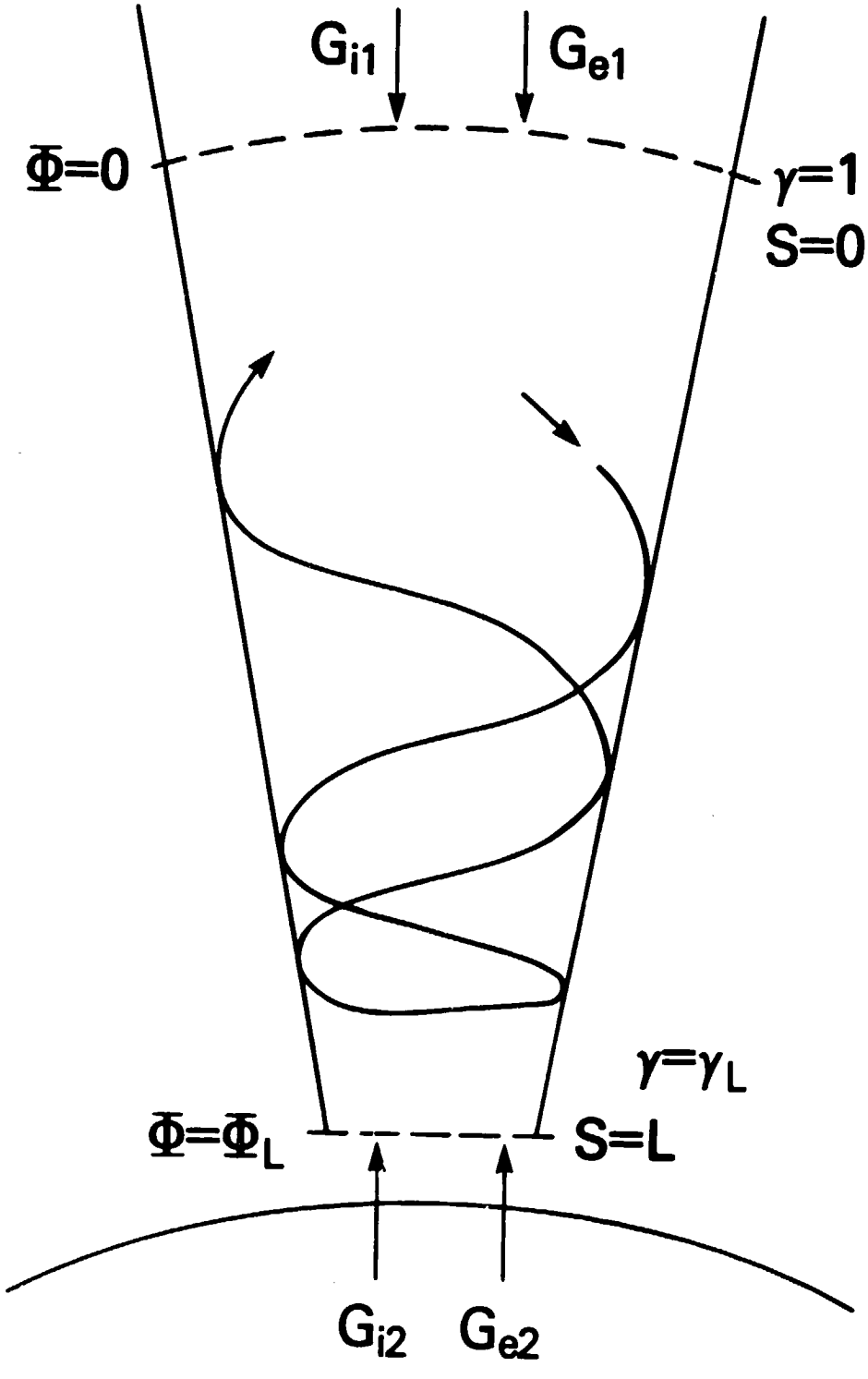

Figure 6

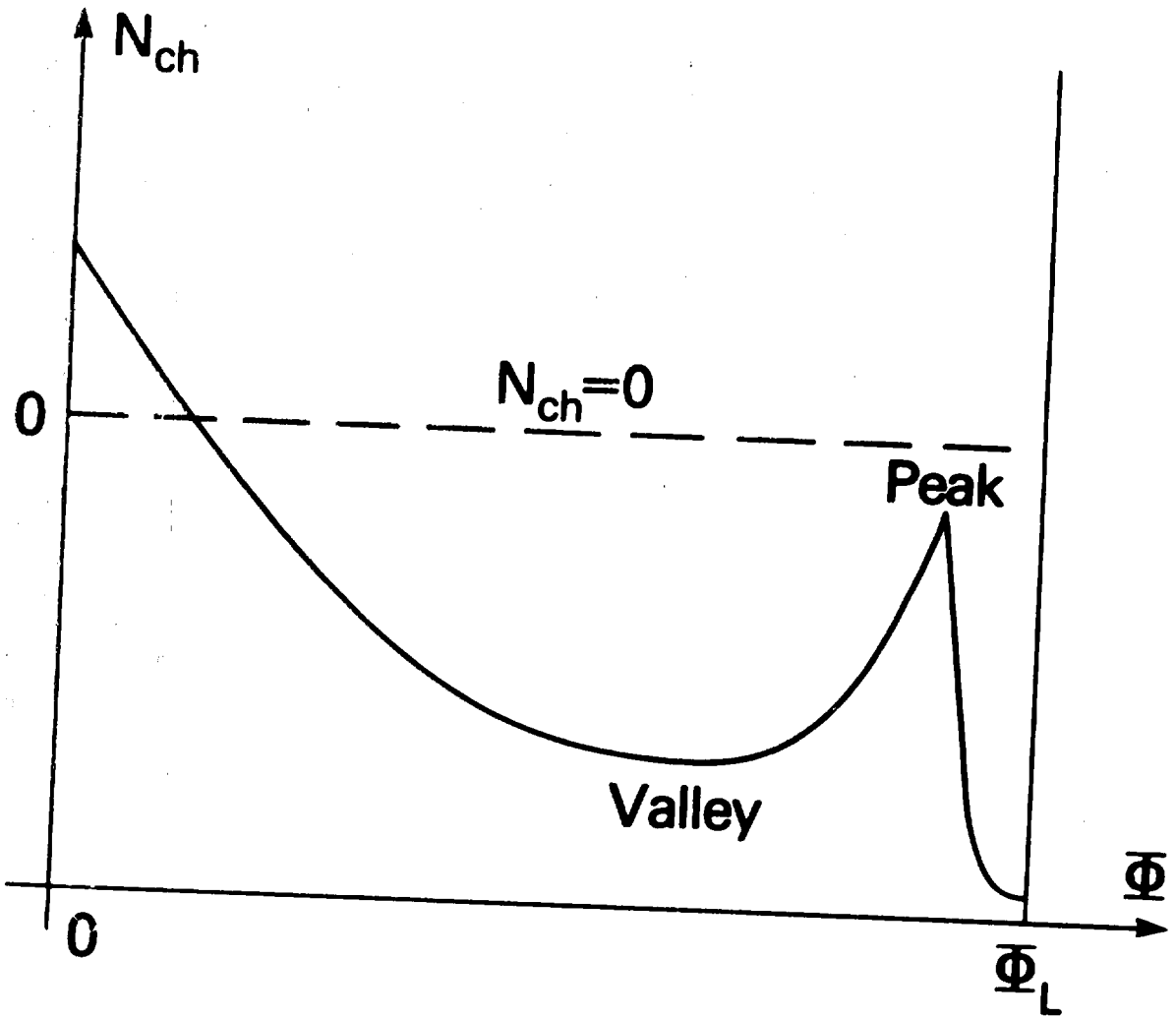

Figure 7

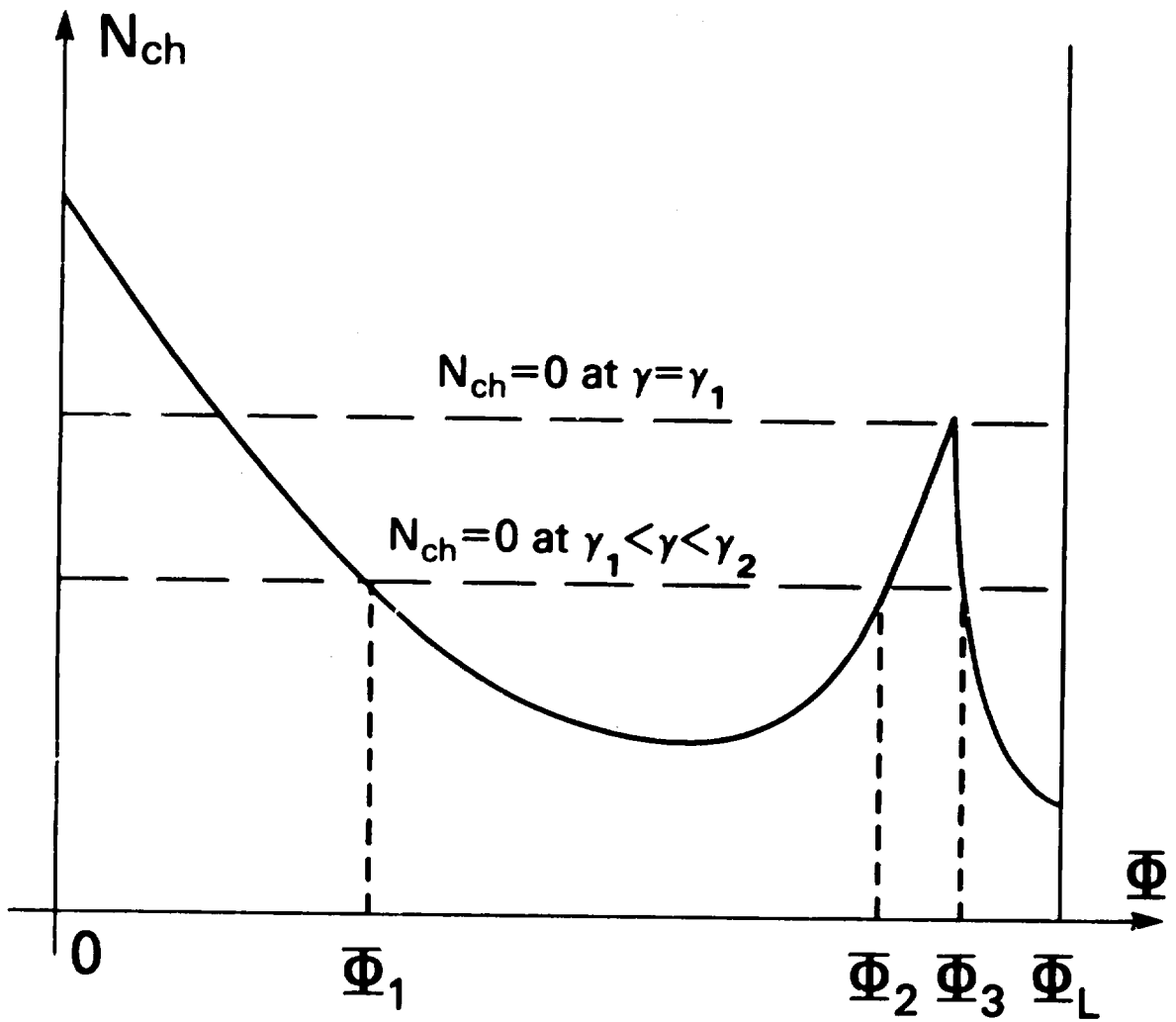
N_{ch}
$N_{ch}=0$ at $\gamma=\gamma_1$
$N_{ch}=0$ at $\gamma_1<\gamma<\gamma_2$
Φ
0
Φ_1
Φ_2 Φ_3 Φ_L

Figure 8

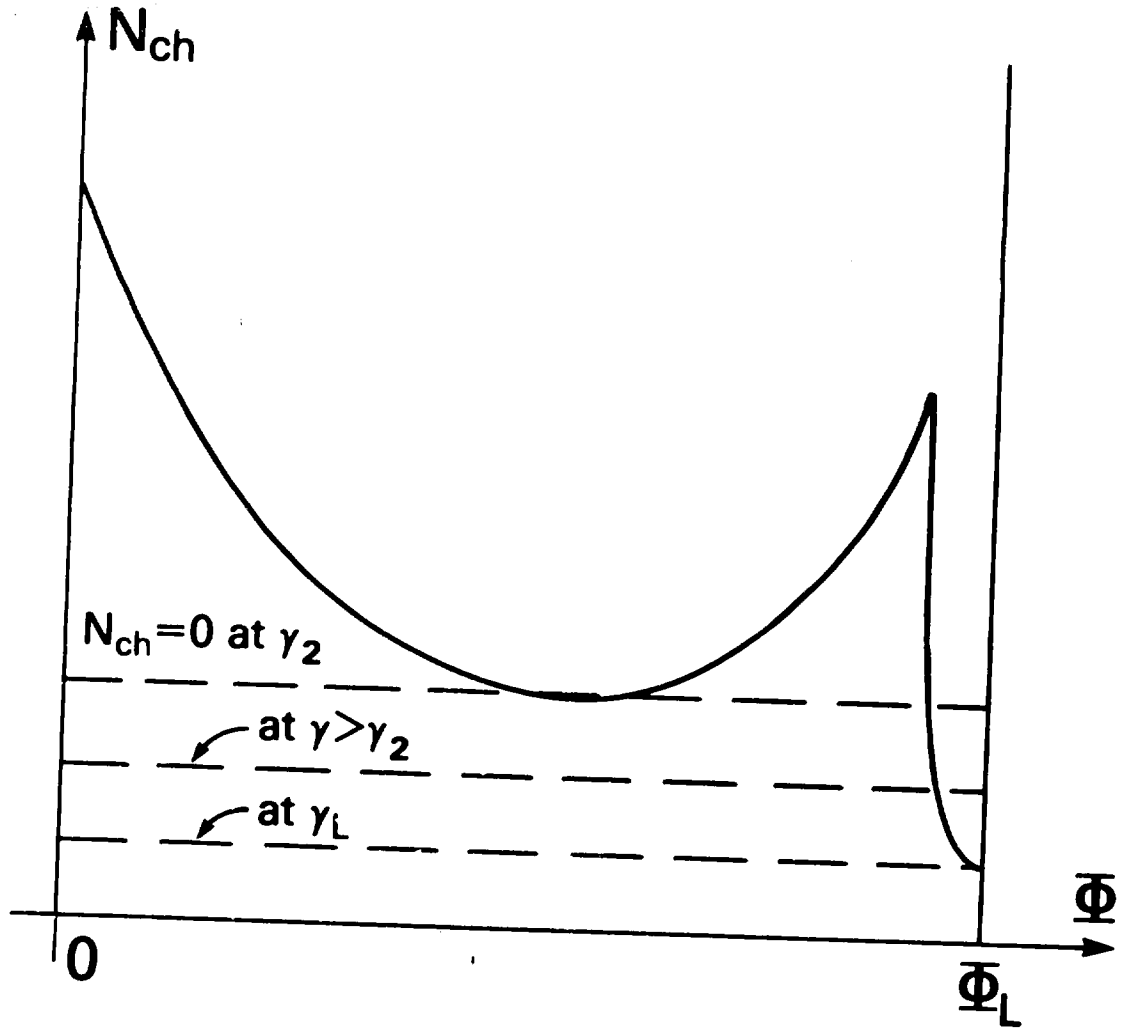

Figure 9

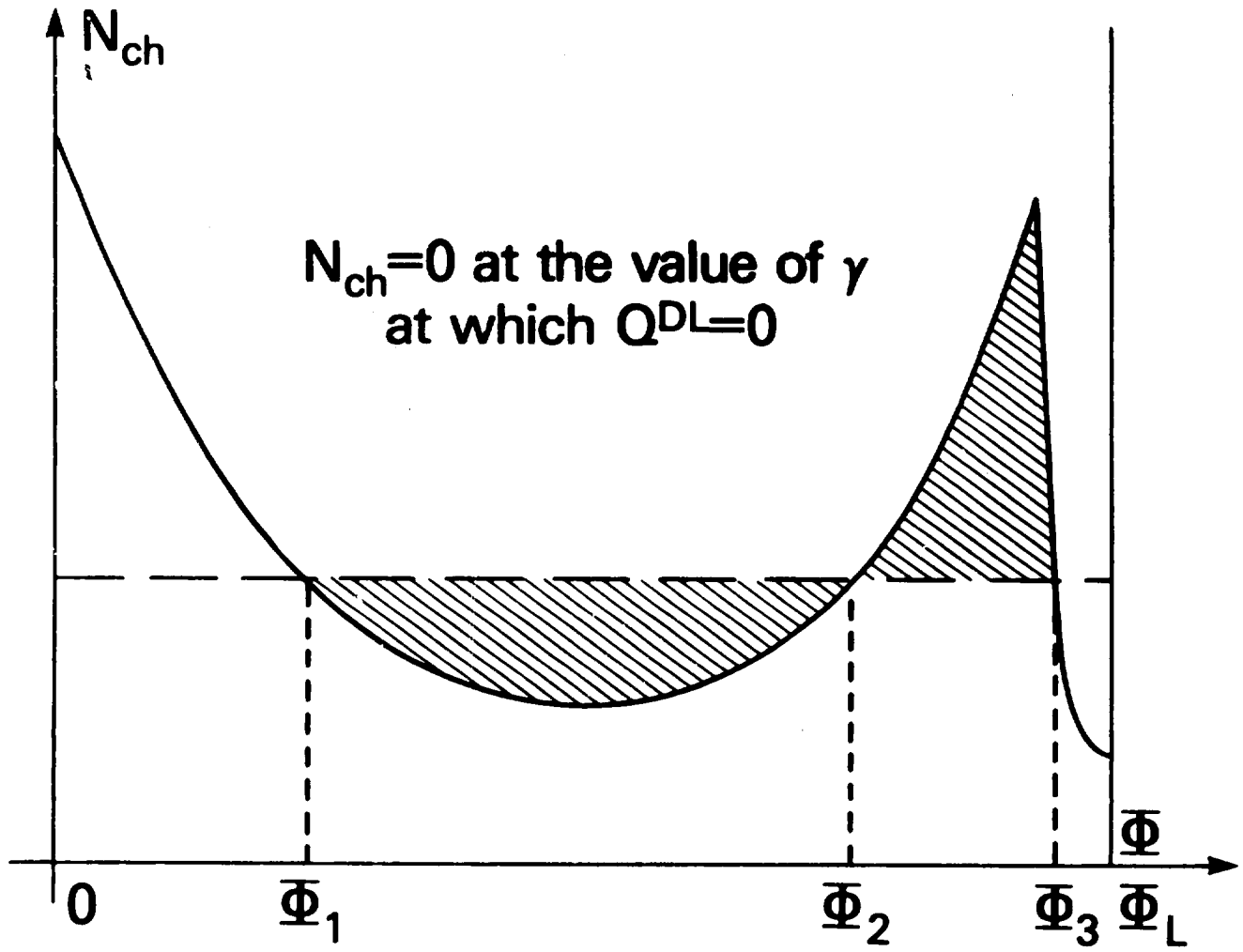
N_{ch}
N_{ch}=0 at the value of γ
at which Q^{DL}=0
Φ
0
Φ_1
Φ_2
Φ_3
Φ_L

Figure 10

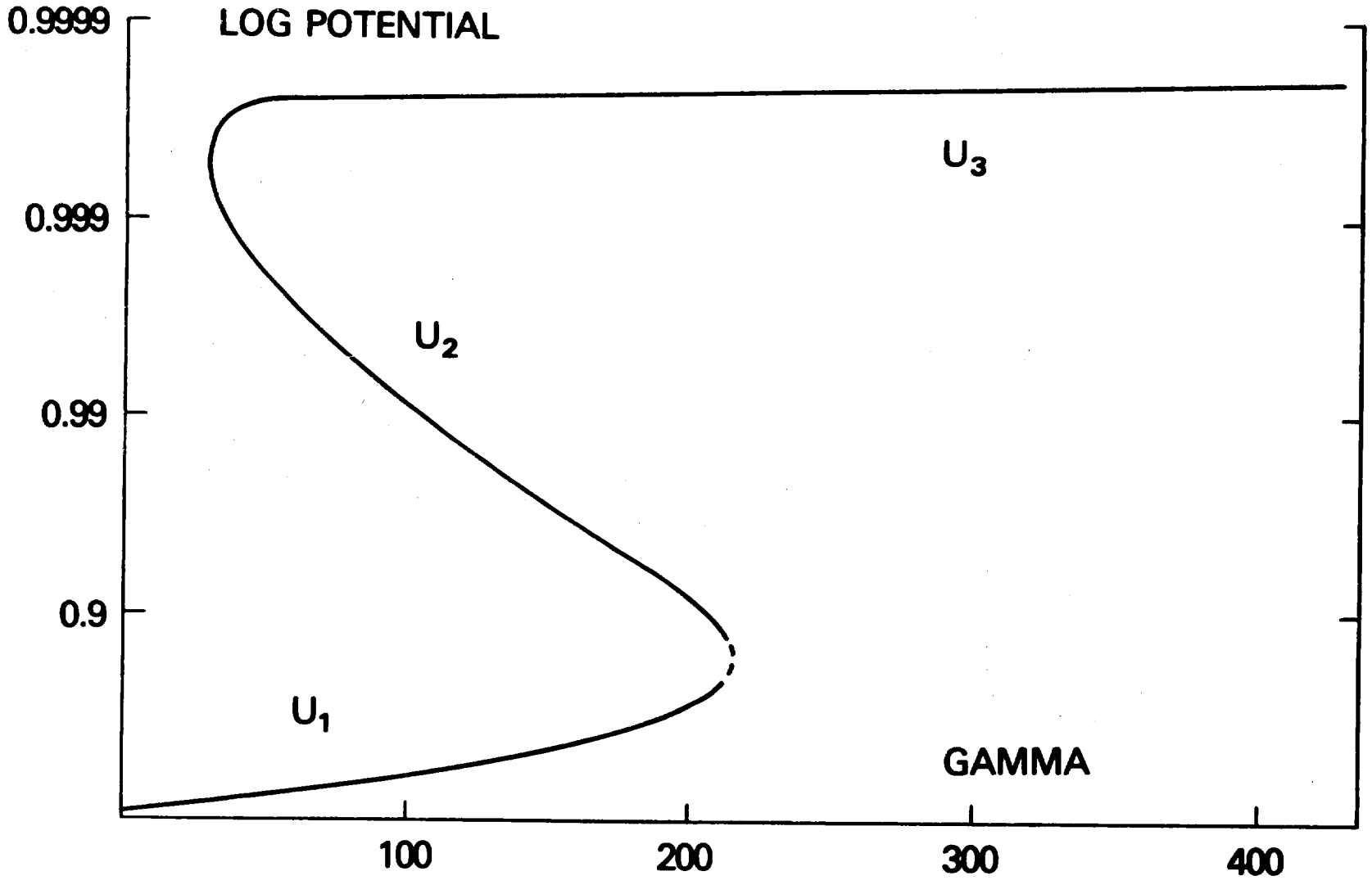

Figure 11

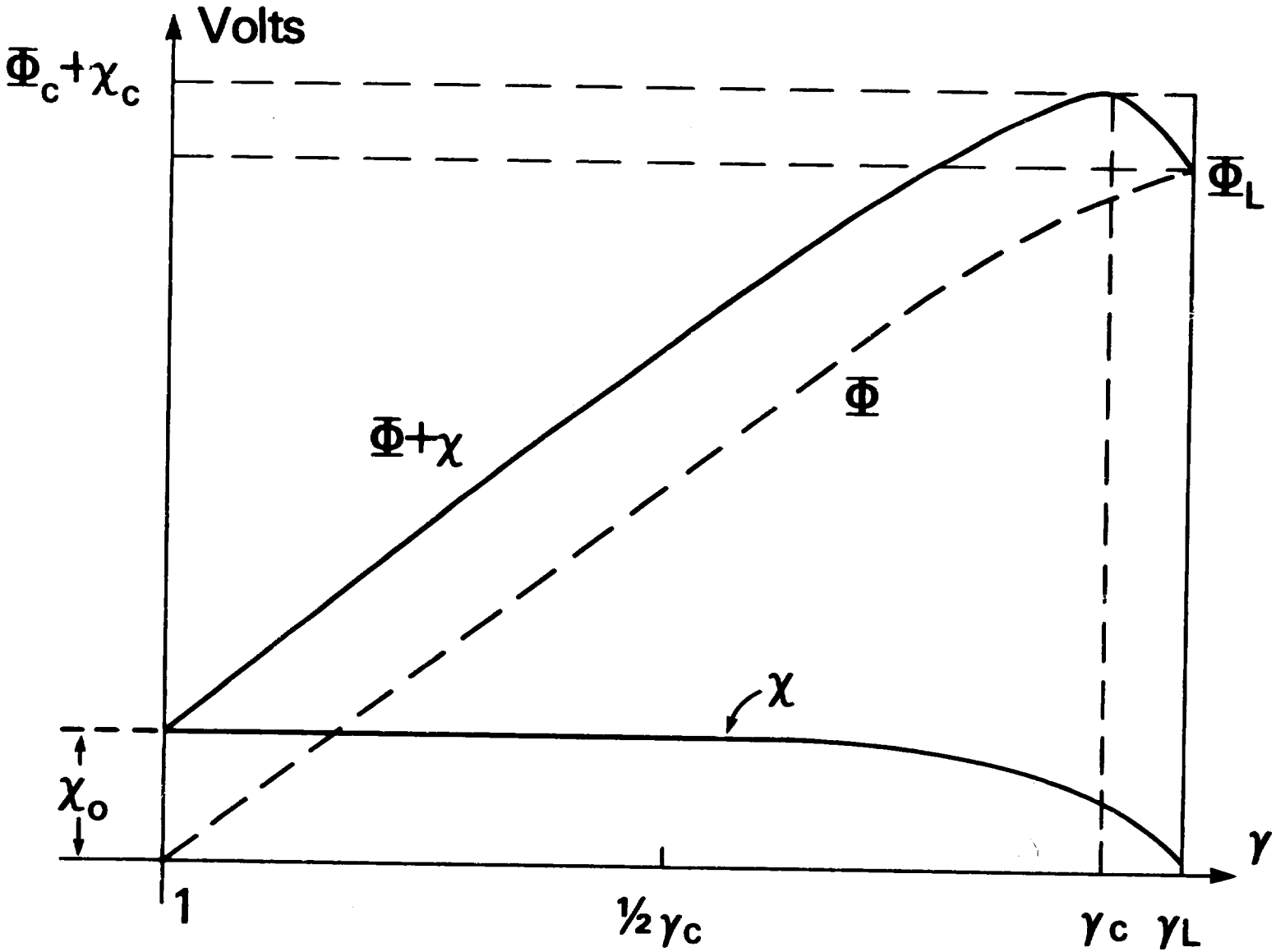
Volts
$\Phi_c+\chi_c$
Φ_L
$\Phi+\chi$
Φ
χ
χ_o
1
$\frac{1}{2}\gamma_c$
γ_c
γ_L
γ

Figure 12

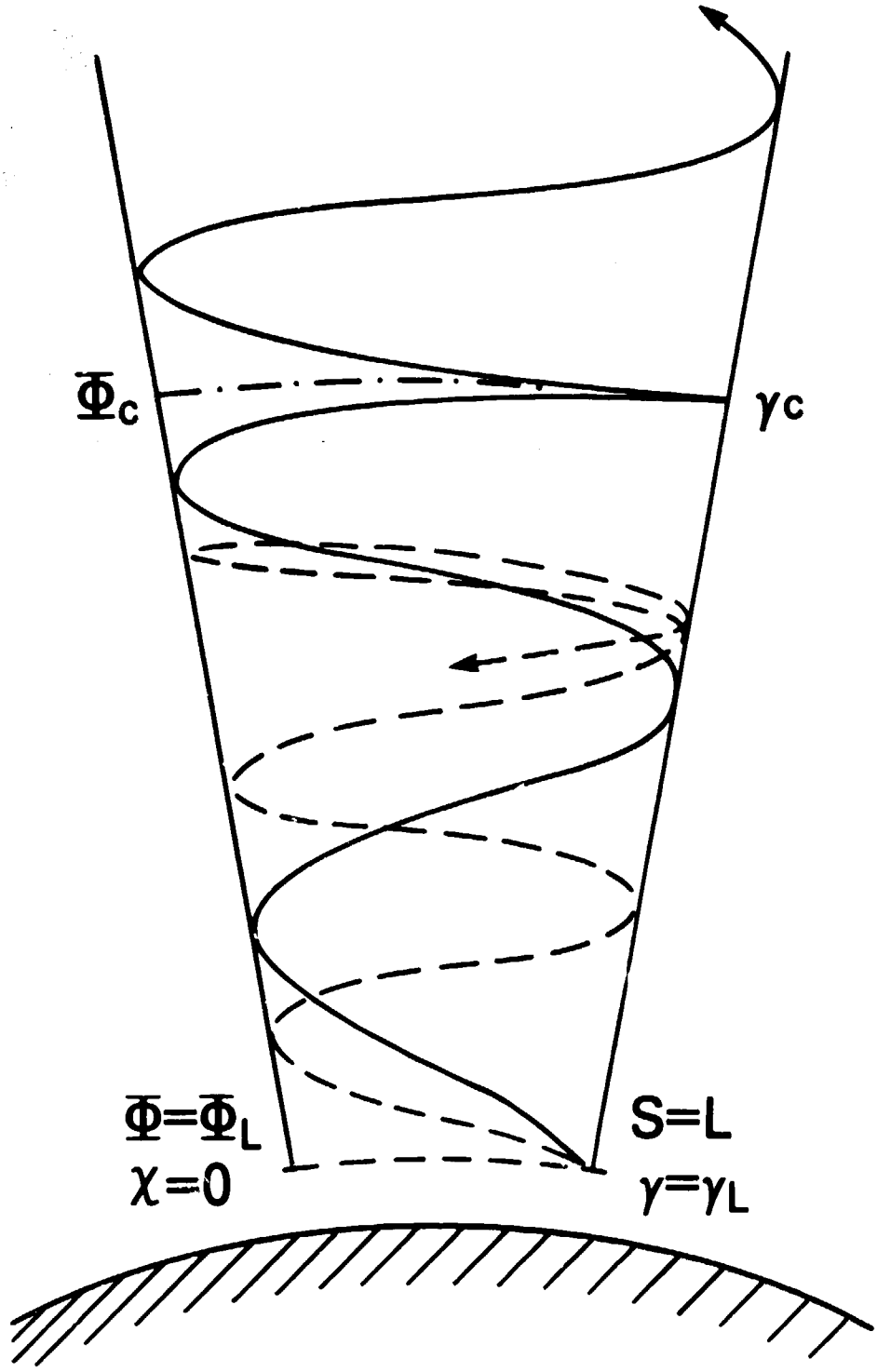

Figure 13

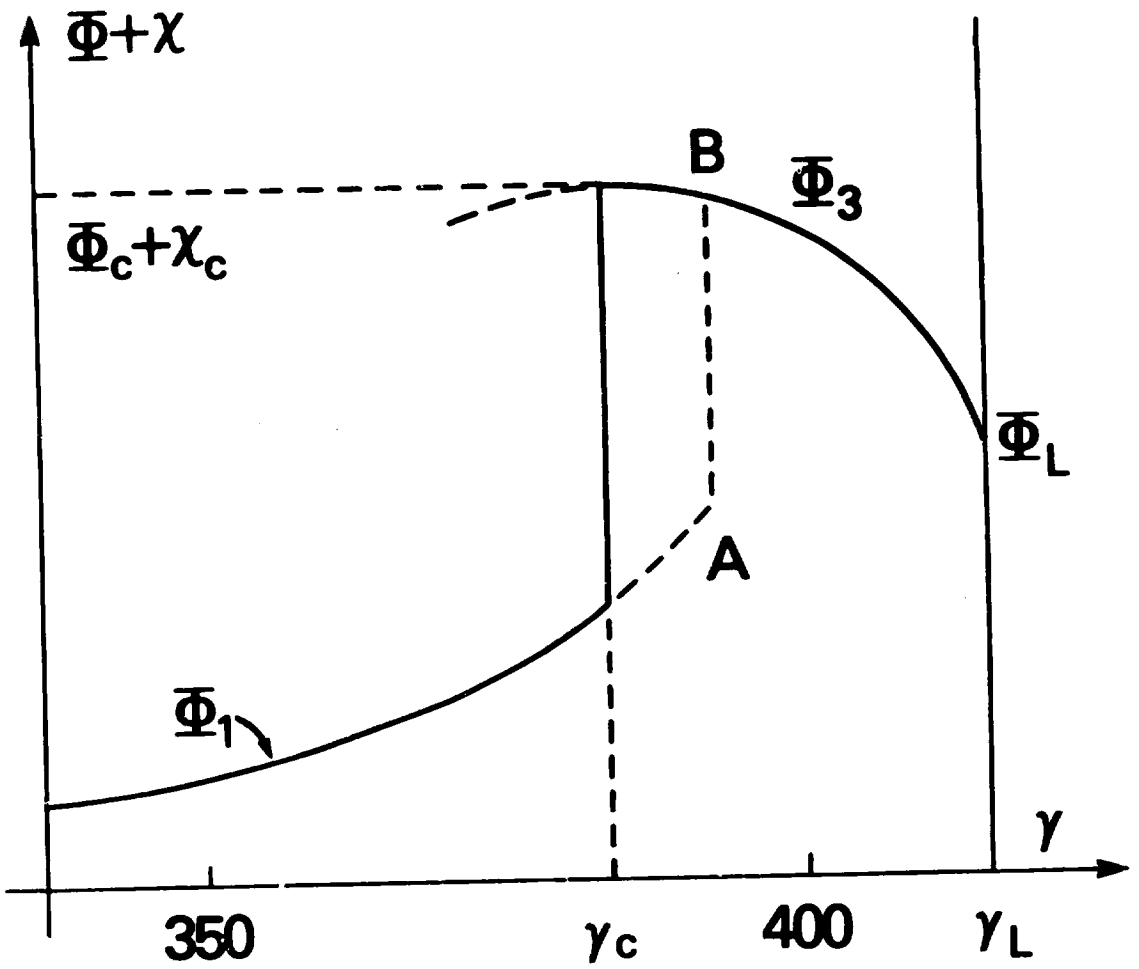

Figure 14

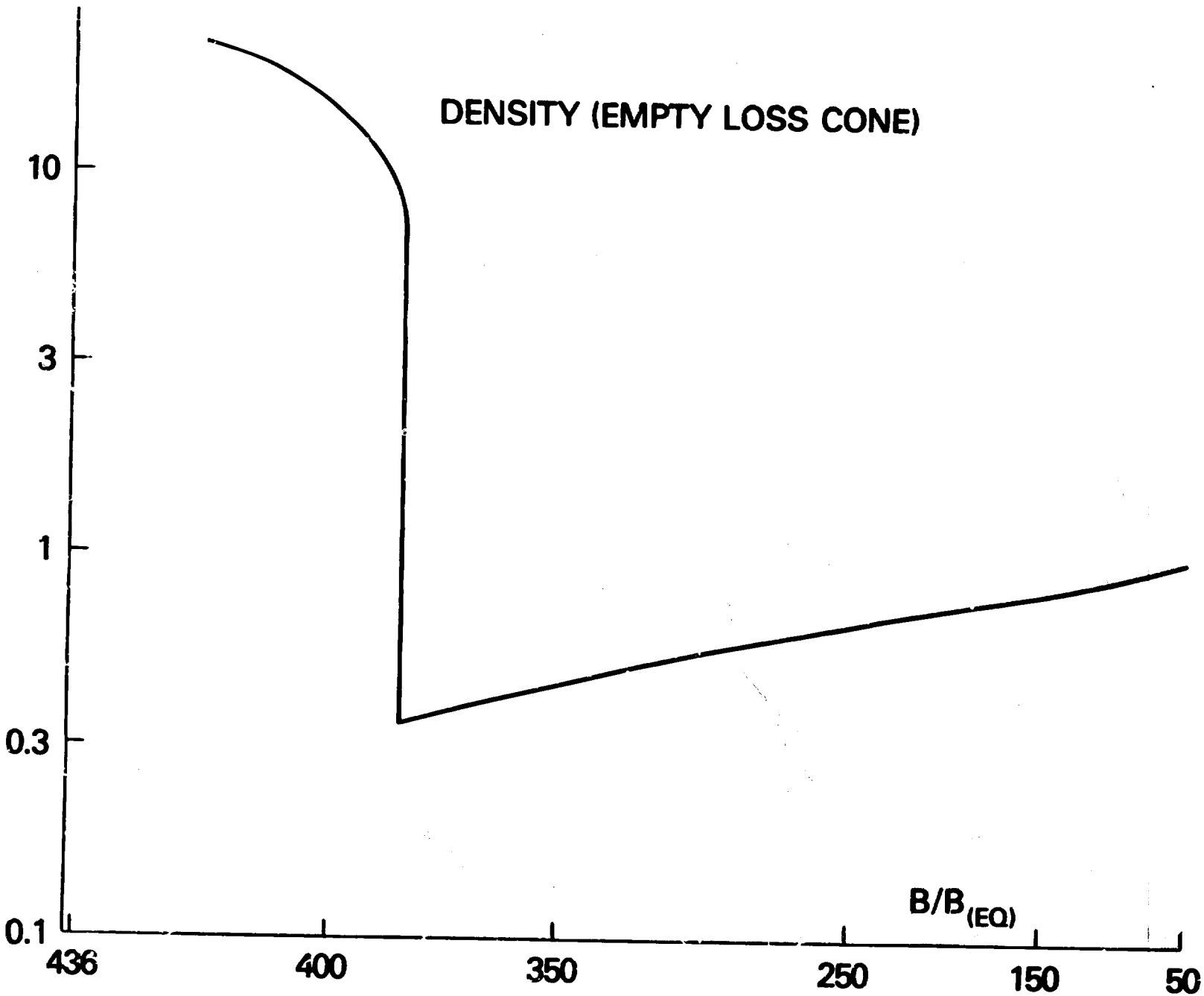

Figure 15

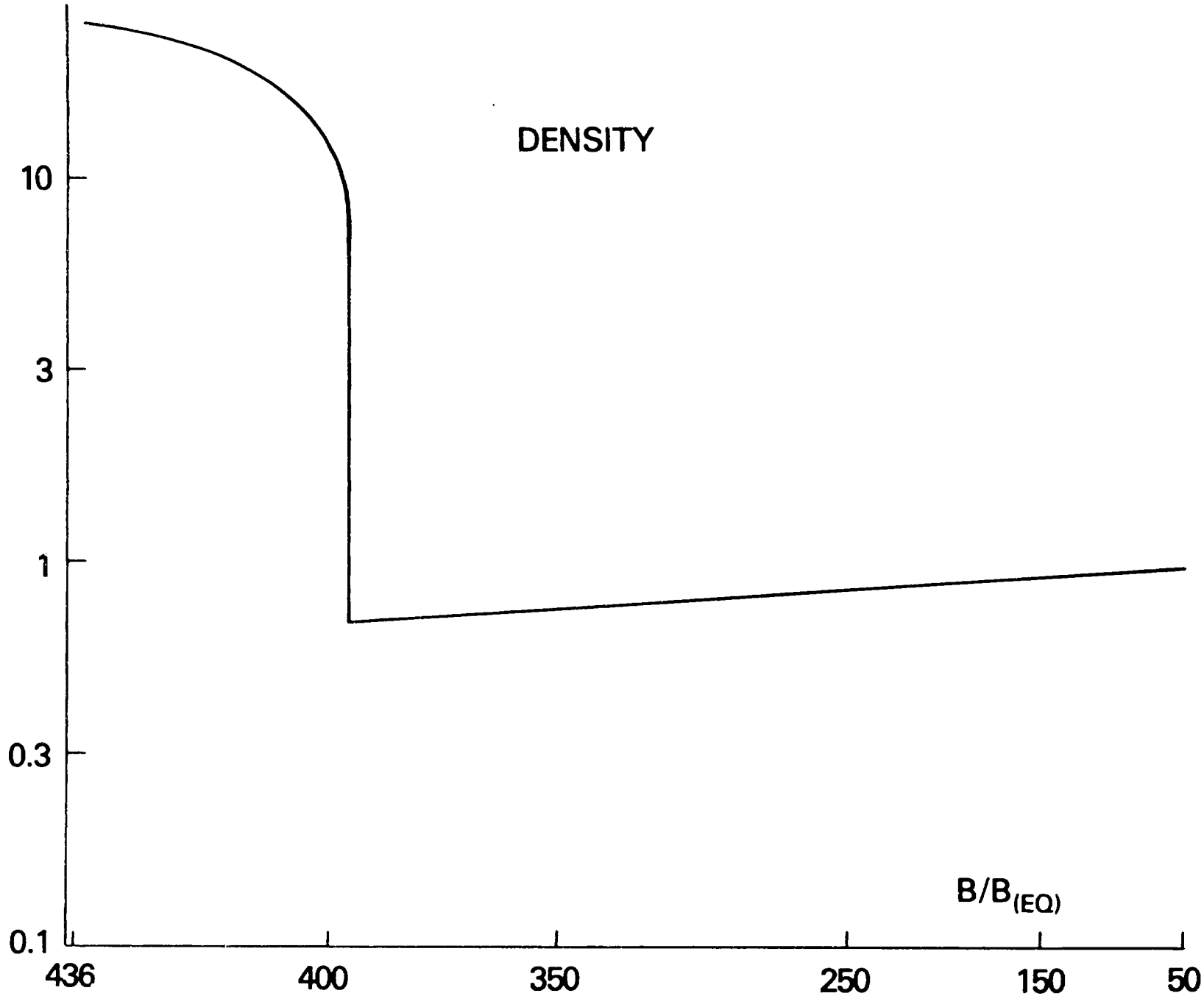

Figure 16